

**COMBINED COOLING AND
BIO-TREATMENT OF BEET-SUGAR
FACTORY CONDENSER
WATER EFFLUENT**

by George O.G. Löf

June 1971

Completion Report Series
No. 28

COMBINED COOLING AND BIO-TREATMENT
OF
BEET SUGAR FACTORY CONDENSER WATER EFFLUENT

Completion Report
OWRR Project No. A-008-COLO

by

George O. G. Lof,
John C. Ward,
O. J. Hao

Department of Civil Engineering
Colorado State University

submitted to

Office of Water Resources Research
U. S. Department of Interior
Washington, D. C. 20240

June 30, 1971

The work upon which this report is based was supported (in part) by funds provided by the United States Department of the Interior, Office of Water Resources Research, as authorized by the Water Resources Research Act of 1964, and pursuant to Grant Agreement No. 14-31-0001-3006.

Colorado Water Resources Research Institute
Colorado State University
Fort Collins, Colorado 80523

Norman A. Evans, Director

TABLE OF CONTENTS

<u>Chapter</u>		<u>Page</u>
I	INTRODUCTION	1
II	REVIEW OF LITERATURE	3
	Cooling Tower Principles	3
	Theory of Biological Treatment	3
	Theory of Trickling Filter	5
	Applications of "Combined Cooling and Bio-treatment"	7
III	BOD AND CHEMICAL ANALYSIS OF CONDENSER WATER EFFLUENT	16
	BOD	16
	BOD Results and Discussion	17
	Chemical Analysis	20
	Theoretical Oxygen Demand (TOD), COD, and BOD Comparisons	22
IV	EXPERIMENTAL EQUIPMENT AND PROCEDURE	26
	Apparatus	26
	Miscellanea	27
	Operating Procedure	30

TABLE OF CONTENTS - Continued

<u>Chapter</u>		<u>Page</u>
V	RESULTS AND DISCUSSION	31
	COD and Nitrogen Removal	31
	Detention Time	41
	Thermal Considerations	46
	Microbiology Study	65
VI	SUMMARY AND CONCLUSION	69
	LIST OF SYMBOLS	73
	BIBLIOGRAPHY	76
	APPENDIX	79

CHAPTER I

INTRODUCTION

Stream pollution from beet sugar factory wastes remains a major problem in at least a dozen states from Michigan west to the Pacific coast (1). Because sugar beet processing is seasonal, discharging wastes often when streams have low flow, the industry has frequently been the target of pollution control investigations. One of the wastes produced by beet sugar refineries is hot condenser water from evaporators and vacuum pans. The concentration of oxygen-demanding materials in this water is generally dependent on the amount of sugar solution droplets entrained in the vapor, which depends on operating conditions and the efficiency of the equipment used. The evaporator condensing wastewater has a low concentration of dissolved organic matter, but its large volume results in significant stream pollution primarily by heat, BOD, and nitrogen. The methods for reducing pollution from lime cake slurry, flume, beet wash, and process water from beet sugar factories cannot be easily adapted to the treatment of condenser water because of its high flow rate, high temperature, and low organic concentration.

A possible method for biological treatment of this wastewater is by use of cooling towers (2, 3, 4, 5, 6, 7). Considerable success has been achieved in the treatment of certain heated effluents from petroleum refineries by use of slightly modified forced draft water

cooling towers. Under suitable conditions simultaneous cooling and biological oxidation of phenol and other organics can be accomplished. This kind of treatment reduces not only thermal and organic pollution, but also the withdrawals of fresh water because of reuse of this treated effluent.

The objective of this study is to appraise the feasibility of reducing both thermal and organic pollution from the condenser water of beet sugar factories by using a cooling tower in a closed system in which biological oxidation of sugars and other organic matter is induced and maintained. This study required the determination of the conditions under which condenser water will undergo biological oxidation, the extent of COD removal which can be achieved under conditions simulating cooling tower operation, and the size of the equipment required.

CHAPTER II
REVIEW OF LITERATURE

Cooling Tower Principles

Evaporative cooling of water involves the continuous contact of air and water accompanied by heat and mass transfer. Large surface areas of water are provided by distributing the warm water over packing that allows the water to flow downward in thin films. The water is thus cooled by exchange of sensible and latent heat between the water and a stream of relatively cool, dry air. The rates of heat and mass transfer depend on driving potentials. Because both mass and heat are transferred by similar mechanisms, the ratio of heat transfer coefficient to mass transfer coefficient is approximately constant.

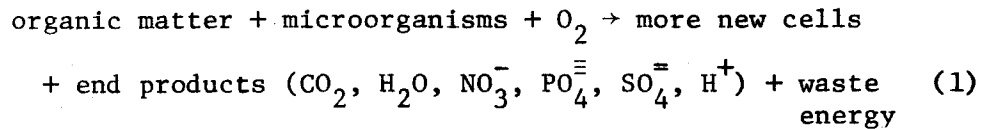
Part of the mass transfer data available from experimental work in cooling towers is summarized in Table I. Because the relations shown are empirical results of experimental data, they should not be extrapolated beyond the range of the data.

Theory of Biological Treatment

The operation of any biological wastewater treatment process depends upon the biological action produced by the microorganisms in the treatment system. The biological growth clinging to the media surface contributes to stabilizing the adsorbed organic pollutants present in wastewater as follows:

Table 1: Experimental Mass Transfer Rates for Contact of a Pure Liquid with a Gas

Item	Equipment	Process and notes	Range of flow rates $\left(\frac{\text{lb}}{(\text{hr})(\text{ft}^2)}\right)$	Equation	Reference
1	10 inch diameter tower; 12.5 inch depth of 15, 25, 35 mm Raschig rings	Humidification-cooling, liquid cooling, and dehumidification with air-water	$200 \leq L \leq 4,160$ $137 \leq G \leq 586$	$K_{Y^a} = 0.45 G L^{0.2}$	8
2	21.5 inch square tower, 1 1/2 inch Berl saddles	Humidification-cooling with air-water. Corrected for end effects	$120 \leq L \leq 6,800$ $100 \leq G \leq 700$	$K_{Y^a} = 1.25 G^{0.39} L^{0.48}$ $K_Y = 0.0283 G^{0.39} L^{0.48}$	9
3	6 foot square tower, 11.25 feet packed height, wood slats, 3/8 x 2 inches, spaced parallel, 15 inches between tiers	Liquid cooling with air-water	$350 \leq L \leq 3,000$ $664 \leq G \leq 1,680$	$K_{Y^a} = 0.197 L^{0.4} G^{0.5}$	10
4	41 5/8 x 23 7/8 inch tower, packed height = 41 3/8 inch. Wood slats, 1/4 x 2 x 23.5 inches, bottom edge serrated, on 5/8 inch horizontal centers, 3 5/8 to 2 5/8 inch vertical centers. 18 spray nozzles.	Liquid cooling with air-water	$880 \leq L \leq 1,500$ $700 \leq G \leq 1,500$	$K_{Y^a} = 0.00029 L G - 0.114 G$ $- 0.133 L + 311$	11



Equation 1 is for aerobic conditions in which dissolved oxygen exists in the wastewater. This basic metabolic process may be divided into two phases which proceed simultaneously.

1. Synthesis; conversion of organic matter into new cells
2. Oxidation; conversion of organic matter to energy for use in synthesis.

It is reasonable to assume that factors affecting the activity of enzymes, such as pH, temperature, heavy metals, antimetabolites, toxic organics, concentration of enzymes, and concentration of organic matter, influence the biological growth response which correspondingly affects the biological treatment.

Theory of Trickling Filter Operation

Trickling filters are used widely in biological treatment of sewage and industrial wastewater. Traditionally, a trickling filter was merely a pile of rocks through which wastewater passed slowly. Removal of the organic matter in the applied wastewater is the result of an adsorption process that occurs at the surface of the biological slimes covering the filter media (12). Subsequent to their adsorption and absorption, the organics are utilized by the slimes for growth and energy. Fair and Geyer (13) state: "The use of trickling filters and activated sludge for the treatment of organic wastewaters is based upon the capacity of the microorganisms living in the system to (1) abstract needed food substances from wastewater, and (2) to elaborate gelatinous films that, together with the organisms themselves, constitute the

essential elements of an aerobic biological treatment system. Because of their viscous jelly-like nature and their microbial population, these films are called zoogloal films. These biological creations possess the signal ability to (1) transfer to themselves, among other things, energy-yielding substances that were dissolved or suspended in the carrying water, and (2) to release to the water some of the end products of their metabolism including water, carbon dioxide, nitrate, and sulfate. The mechanism involved in the exchange of substances from and to the carrying water are complex and variable."

In the past two decades, there have been many attempts to replace the rocks of trickling filters with packings of coke, slag, wood, ceramic shapes, and various synthetic plastics (14). Studies also have been made of nozzle arrangements, distribution systems, wastewater application rates, and other aspects of the overall design. Application of the results of these studies has resulted in improved performance of trickling filters.

Theoretical considerations show that the rate of removal of organic matter is related to the surface area of organic matter within the filter. Inasmuch as the contact time within a given filter is related to its depth, it has been possible to set up the basic equation in units of time or units of depth. A purification relationship, which approximates a first-order reaction, with or without retardation, is given by Fair et al (15) as follows:

$$\frac{dy}{dt_d} = k \left(\frac{y_o - y}{y_o} \right)^n (y_o - y) \quad (2)$$

where

y_o is the initial or removable concentration of substances present in the applied wastewater

y is the amount removed during passage through the treatment unit (vertically in trickling filters)

t_d is the detention time within the unit

k is a proportionality factor with the dimension (time)⁻¹

n is a measure of the degree of dropoff in treatment response or the retardation during the progress of purification.

Applications of "Combined Cooling and Bio-treatment"

As early as November, 1954, the Sun Oil Company refinery in Toledo, Ohio (2, 3, 4, 7) achieved double duty from its forced-draft redwood cooling towers by using them as biological filters to reduce wastewater pollution. The 90° to 100°F wastewater temperature, extensive internal contact surface, and excess oxygen provided optimal environmental conditions for mesophilic biological activities. Bacteria, thriving on the contact surface, oxidized and destroyed phenols, sulfides, and mercaptans, and reduced the chemical oxygen demand of the wastewater.

After this initial phase, engineers at Sun Oil Company believed that consistently high biological removal efficiencies could be maintained. Consequently, their cooling system was expanded greatly. In mid 1957, a total pumping capacity of 3,000 gpm was installed so that

all of their wastewater could then be pumped to the cooling towers as makeup for the system. Successful biological treatment was accomplished. Four cooling towers, two forced-draft and two induced-draft, have been utilized on this wastewater ever since.

Water inlet and outlet temperature ranged from 70 to 120°F and 64 to 90°F, respectively, in both forced-draft and induced-draft cooling towers. Efficiency of bio-adsorption of phenolic type compounds as shown in table 2 normally exceeded 99.9 percent. BOD and COD removal were 90 and 80 percent, respectively.

In 1956, the A.E. Staley Manufacturing Company (5) of Decatur, Illinois, tested a system for simultaneous cooling and biological purification of heated wastewater from a corn milling operation. This process involved the use of a synthetic polystyrene medium in an experimental forced-draft cooling tower 3 by 3 by 14 feet tall. It was hoped that the synthetic packing would serve both as cooling area and as a surface upon which biological growth would develop. Later studies of this small tower showed good cooling efficiency and purification. In 1958, they constructed a three-section induced-draft cooling tower (32 by 74 by 74 feet) in one section of which the polystyrene medium was used in place of the common redwood packing. Performance data showed this tower cooled wastewater from 120° to 85°F under summer conditions at the rate of 7 mgd. The biological media were found capable of removing 300 pounds BOD per 1,000 cubic feet of filter media per day at a liquid rate of 3 gpm per square foot.

Table 2: Phenolic Compound Removal Data for Forced and Induced Draft Cooling Towers, Sun Oil Company, Toledo, Ohio (Reference 7)

Sample Location	Phenolic-Type Compounds			% Removal	Flow GPM	Type of Cooling Tower
	mg/l	lbs/day	lbs/day Removed			
Makeup	48.0	346			600	Forced Draft
Blowdown	0.082	0.099	345.9	99.9+	100	
Makeup	70.0	840			1000	Forced Draft
Blowdown	0.41	2.46	837.5	99.7	500	
Makeup	15.7	133			710	Forced Draft
Blowdown	0.194	0.23	132.8	99.8	100	
Makeup	19.6	141			600	Forced Draft
Blowdown	0.800	0.96	140	99.4	100	
Makeup	17.2	165			800	Induced Draft
Blowdown	0.115	0.31	164.69	99.8	225	
Makeup	10.0	102			850	Induced Draft
Blowdown	0.033	0.109	101.89	99.9	275	
Makeup	13.2	146			925	Induced Draft
Blowdown	0.033	0.133	145.87	99.9	350	
Makeup	33.2	364			910	Induced Draft
Blowdown	0.043	0.196	363.804	99.9+	370	

(Table 2 continued)

Chemical Oxygen Demand Reduction for Forced and Induced Draft
Cooling Towers, Sun Oil Company, Toledo, Ohio (Reference 7)

Sample Location	Chemical Oxygen Demand			% Removal	Flow GPM	Type of Cooling Tower	Ratio: <u>makeup lbs/day</u> blowdown lbs/day
	mg/l	lbs/day	lbs/day Removed				
Makeup	331	2,390			600	Forced Draft	14.14
Blowdown	141	169	2,221	93.1	100		
Makeup	389	2,802			600	Forced Draft	12.08
Blowdown	194	232	2,570	91.8	100		
Makeup	233	2,790			1000	Forced Draft	3.83
Blowdown	133	728	1,992	71.4	500		
Makeup	301	3,610			1000	Forced Draft	4.25
Blowdown	142	850	2,760	76.3	500		
Makeup	488	4,683			800	Induced Draft	2.96
Blowdown	587	1,584	3,099	66.2	225		
Makeup	771	8,555			925	Induced Draft	5.70
Blowdown	372	1,500	7,055	82.5	350		
Makeup	705	6,765			800	Induced Draft	4.16
Blowdown	551	1,628	5,137	75.8	245		
Makeup	953	10,415			910	Induced Draft	3.96
Blowdown	586	2,607	7,808	75.0	370		

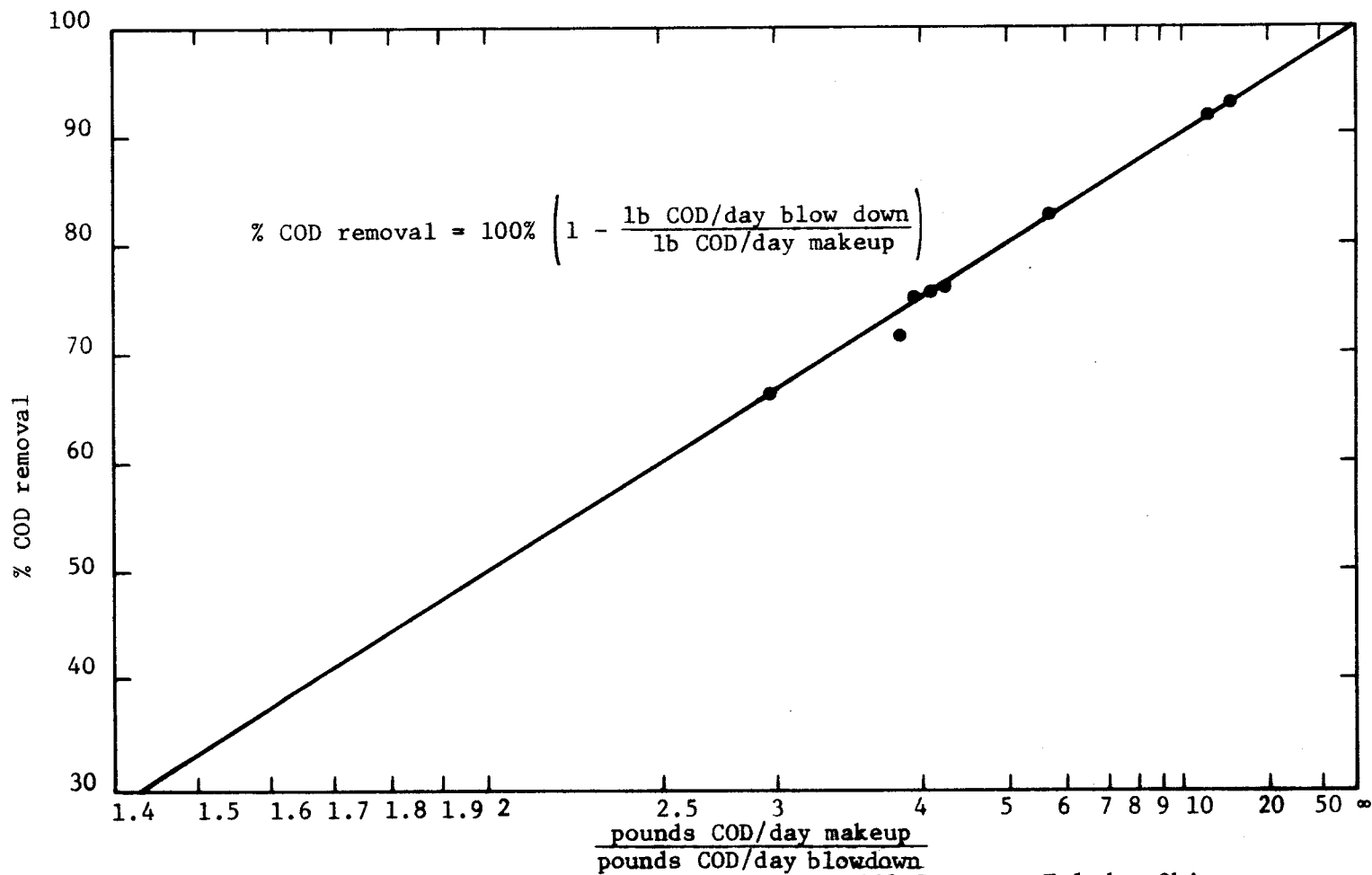


Figure 1: COD removal in cooling towers, Sun Oil Company, Toledo, Ohio.

In 1960, it was reported (16) that the Fluor Corporation, Ltd, Los Angeles, California, had developed a plastic packing for use in trickling filters. This was the first "engineered" use of a cooling tower, splash-type medium for biological oxidation. The performance of this particular packing was good. It was concluded that much of the BOD reduction in a system containing a splash-type packing was due to the biological growth on the packing. The drops formed provided a large surface area for the absorption of oxygen and resulted in a continuous oxygen supply for biological treatment. One interesting point was that the biological media did not grow on the top of packing decks. Growth was confined to the vertical section of the packing decks and did not extend out beyond the protective overhang of the T-strips. This was probably due to the high hydraulic loadings used during operation, which should reduce the possibility of the packing being plugged or fouled by excessive biological growth.

In the summer of 1962, a study was conducted by Hydrosience Inc. (6) in which two synthetic media towers were operated in parallel for the dual function of biological oxidation and cooling of wastewater from the production of bleached board and corrugating medium. Both towers were operated with mechanical draft equipment. The BOD removal for the two media at the rate of 3 gpm per square foot hydraulic load was about 30 percent. The cooling that was achieved in both systems was quite efficient with one achieving a 14.5°C decrease and the other achieving a 7.5°C decrease when operated at a 42°C inlet wastewater temperature.

Another board mill in Pennsylvania also used this medium for dual purpose treatment in a pilot plant (6). Removal of 50 percent

of the applied BOD was achieved when operating at a 1.2:1 recirculation ratio and a total flow rate of 6 gpm per square foot. Although heavy sliming occurred on the packing of this unit, growth was never sufficient to cause any problem in the operation of the tower.

In the pulp and papermill industry (17), an attempt to simultaneously reduce the temperature of wastewater and remove organic matter by use of activated sludge was successful. This pulp mill used a combination of a plastic medium trickling filter and the activated sludge process, wherein return activated sludge would be recycled through the trickling filter with the feed stream. Besides the reduction of BOD, the process also provided a rapid reduction in the temperature of the system by the cooling tower effect of the trickling filter and predilution with cool recycled water.

In 1965, a film factory (18), whose effluent contained highly corrosive alcohol-based solvents, installed three plastic cooling towers in series. The effluent reached the first tower at a temperature of approximately 120°F, and left the third one at approximately 90°F. During passage through the series of cooling towers, the solvent contamination was reduced by some 75 percent. The installation was arranged so that the overflow from the first tower fell by gravity into the second, and from the second into the third. Each tower was equipped with an individual recirculating pump running at maximum rate for that tower. During passage through the first tower, a great deal of the solvent was evaporated while the effluent was cooled. In the remaining

two towers, additional cooling and aeration of the wastewater took place. Bacterial growth was found on the fill during their operation. The glass fibre casings of the plastic towers proved to be resistant to the corrosive effects of the solvents.

Aeration ponds, operated with long detention times in biological wastewater treatment, can also provide a satisfactory temperature reduction. The following experiments in pulp and paper plants are examples.

1. A kraft linerboard mill in Springfield, Oregon (19), has shown satisfactory BOD reduction and temperature decrease in an aeration pond. Inlet temperature ranged from 85 to 105°F, while wastewater temperatures ranged from 64 to 86°F in the aeration pond. During the colder part of the winter season, when the aeration basin temperature averaged 67°F, BOD reduction was 90.7 percent. During the summer in 1966, the basin temperature averaged 80°F, and BOD reduction was 92.8 percent. This very effective method of reducing BOD loading had more than achieved the expected goal of removing 4,000 lbs of BOD per day in a 1,050 ton unbleached kraft linerboard mill.

2. Another pulp mill in Kamloops, Vancouver, B.C., Canada, (19) also had a 92 percent BOD reduction in its aeration pond in the summer season with a pond outlet temperature of 84°F. In the winter the efficiency dropped to 85 percent at a pond outlet temperature of 68°F. The average BOD before treatment was equivalent to 15,000 pounds per day, and the water requirement for the mill was 13 mgd.

3. Cooling by aeration reduced the temperature of wastewaters at a pulpmill in Cosmopolis, Washington, (19) where the influent temperature

averaged 113°F. Reduction of BOD ranged from 83 to 95 percent. Overall average efficiency had been 86 percent with influent BOD ranging from 20,000 to 200,000 pounds per day at an average concentration of 4,000 mg/l.

CHAPTER III
BOD AND CHEMICAL ANALYSIS OF
CONDENSER WATER EFFLUENT

Heated condenser water and raw water were obtained from the Great Western Beet Sugar Factories at Longmont and Loveland, Colorado. Some samples were obtained by "grab" sampling, others by hourly sampling and mixing, to yield composite 24-hour average samples. The composition of the samples varied with the sampling method and time of collection. The automatic sampler gave less gross sediment than hand sampling. Because a beet sugar factory has varying wastewater flow rates during a 24-hour period, one would expect a varying composition.

Before beginning the pilot plant experiments, it was necessary to analyze the Biochemical Oxygen Demand (BOD) characteristics under conditions of various temperature and nutrients, and determine the following water quality parameters: pH, Total Dissolved Solids (TDS), Chemical Oxygen Demand (COD), Nitrogen, and Phosphate.

BOD

The mathematical representation of the BOD reaction is as follows:

$$y = L [1 - \exp (-kt)] \quad (3)$$

where

y is the oxygen demand exerted in time t, mg/l

k is the BOD rate constant, days⁻¹

L is the initial or first-stage BOD of the wastewater, mg/l

t is the time in days.

The BOD reaction is approximately represented by a first order reaction formula as shown in equation 3. The rate of BOD exertion is dependent upon the concentration of biologically oxidizable organic matter present. If the dissolved oxygen (DO) concentration is greater than 4 mg/l at 20°C (20), the BOD exertion rate is independent of the oxygen concentration. This means that the rate-determining step in the reaction is not the step involving DO concentration. The amount of DO measured in condenser water from the beet sugar factory varied from 3.5 to 5.8 mg/l at room temperature. This value almost fits the above assumption that the DO is larger than 4 mg/l. Thus the BOD reaction in condenser water from a beet sugar factory may be considered first order, and dependent only on the concentration of biologically oxidizable matter and on the characteristics of the system which influence the reaction rate constant (temperature, pH, etc.).

BOD Results and Discussion

Measurements of BOD concentration in raw water and condenser water were made by use of Hach manometric equipment (Model 1791) at various temperatures with $(\text{NH}_4)_2\text{HPO}_4$ as nutrient and domestic sewage as a seeding agent. The data are shown in Table 3.

It may be observed that the addition of 1.3 mg/l $(\text{NH}_4)_2\text{HPO}_4$ as nutrient has no effect on the 5-day BOD at all temperatures tested. The explanation, as shown later, is the high nitrogen content of the condenser water from the beet sugar factory. Because domestic sewage has abundant nutrients as well as microorganisms, the condenser water with sewage (one tenth ratio) has higher BOD values.

Table 3: Effect of Temperature and Additives on BOD Concentration of Beet Sugar Factory Condenser Water

Temperature °C	BOD _{5-day} in milligrams per liter			
	Raw water	Condenser water	Condenser water with 1.3 mg/l (NH ₄) ₂ HPO ₄ as nutrient	Condenser water with domestic sewage Condenser water: sewage = 10:1 (volume ratio)
7	6	19	19	
20	15	37	38	70
30		39.5	40	95
48		52	53	85

Another observation is that the BOD of condenser water with sewage at 48°C is less than that at 30°C. The optimum mesophilic growth of the microorganisms in the sewage is about 37°C, so this would explain the observed lower BOD at 48°C. The BOD at the thermophilic optimum (about 55°C) was not investigated.

The BOD of condenser water resulting from seeding with a one-tenth volume ratio of sewage is calculated as follows:

$$\text{BOD of condenser water} = \frac{\left(\text{BOD of condenser water with sewage} \right) \cdot \left(\text{Volume of condenser water and sewage} \right)}{\left(\text{Volume of condenser water} \right)} - \frac{\left(\text{BOD of sewage} \right) \left(\text{Volume of sewage} \right)}{\left(\text{Volume of condenser water} \right)}$$

For example, at 20°C, the 5-day BOD of the sewage is about 200 mg/l. From Table 3 and the above expression, the BOD of the

condenser water is calculated to be about 55.6 mg/l which is greater than its original value of 37 mg/l. This means that the bacteria in the sewage initiated biological activity that resulted in the higher BOD value.

The BOD reaction rate constant (k) at 20°C calculated by various methods is shown in Table 4. These mathematical and graphical methods of evaluating the BOD rate constant are based on an assumed monomolecular or first-order reaction.

Table 4: First Order BOD Reaction Rate Constants at 20°C.

	Fair's log difference method (21)	Thomas' slope method (22)	Moore's moment method (23)	Lee's method (24)	Sheehy's graphical method (25)	Ward's method (26)
k, days ⁻¹	0.107	0.112	0.160	0.135	0.130	0.172

These constants are based on the first stage carbonaceous BOD, with the exception of Ward's method which is based on total BOD that lasted about 15 days.

Part of the variation in values of k shown above is a result of different assumptions involved in the various methods. Moreover, even the same method (in some cases), yields rate constants which differ for different time intervals. For example, in Sheehy's method, k exhibits the following pattern:

$$k_{1,5} > k_{2,5} > k_{3,5} \dots$$

where

$k_{1,5}$ means the calculation is based on the first day and fifth day BOD, and so on.

It is believed that part of the variation in k might also be due to a high initial oxygen demand (25).

The BOD_{5-day, 20°C} of beet sugar factory condenser water effluent can run as high as 70 mg/l, and as low as 3 mg/l. This difference results primarily from process variation. Higher BOD is generally the result of sugar carryover into the vapor, by entrainment, and spillage of sugar solution within the factory. However, such spillage occurs on a very irregular basis.

Chemical Analysis

The following instruments and methods were used to determine the water quality parameters:

pH (Orion Reserach Model 801), 4 significant figures

Conductivity (Conductivity Bridge Model RC 16 B2), 1% instrumental error

Total Dissolved Solids (Standard Methods, 180°C)

COD (Standard Methods)

Phosphate (Hach Instrument)

Nitrogen (Hach Instrument)

Dissolved Oxygen (Beckman Instrument Model 76), laboratory DO probe

Settleable Matter (Standard Methods)

Total Iron (Hach Instrument).

The data from these chemical analyses are shown in Table 5. The BOD_{5-day, 20°C} values are also shown for comparison with COD analyses.

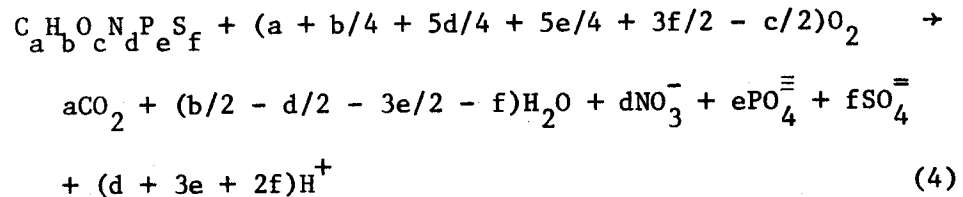
Table 5: Composition of Raw Water and Condenser Water Effluent from a Beet Sugar Factory

	Raw Water			Condenser Water		
	High	Low	Average	High	Low	Average
pH at 20°C	8.1	7.8	7.9	8.7	8.0	8.4
DO at 20°C (mg/l)	6.0	4.5	5.0	5.8	3.5	5.0
Settleable matter (mg/l)	---	---	0.02	0.9	0.1	0.5
TDS at 180°C (mg/l)	810	790	800	856	630	800
NH ₃ -N (mg/l) as Nitrogen	2.3	1.0	1.5	17	8	13
NO ₃ -N (mg/l) as Nitrogen	1.5	0.5	1.0	3.5	1.5	2.0
NO ₂ -N (mg/l) as Nitrogen	0.02	---	0.01	0.5	0.1	0.3
Total Inorganic N	3.82	1.5	2.51	21	9.6	15.3
Ortho-Phosphate (mg/l)	---	---	0.05	---	---	0.05
Total Iron (Fe ⁺⁺ + Fe ⁺⁺⁺) (mg/l)	0.25	0.06	0.1	0.75	0.1	0.5
Conductivity at 25°C (µmho/cm)	1065	1044	1055	1011	942	964
Total C ₁₂ H ₂₂ O ₁₁ *sugar (mg/l)				45.6	22.8	38.0
COD (mg/l)				120	40	85
BOD ₅ -day, 20°C (mg/l)	20	5	14	45	15	37

*sugar data are from equation 6 and COD values.

Theoretical Oxygen Demand (TOD), COD, and BOD Comparisons

The complete oxidation of organic matter can be expressed as follows:



Assuming that the principal impurity in beet sugar condenser water effluent is sucrose, the subscripts in the above equation 4 are probably

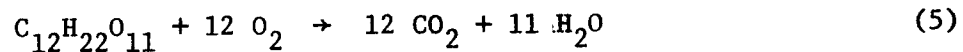
$$a = 12$$

$$b = 22$$

$$c = 11$$

$$d = e = f = 0$$

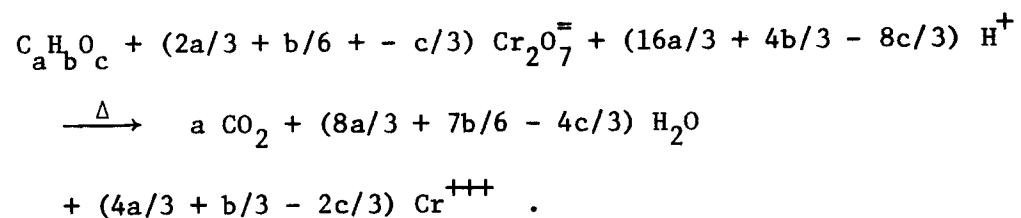
So equation 4 can be rewritten as:



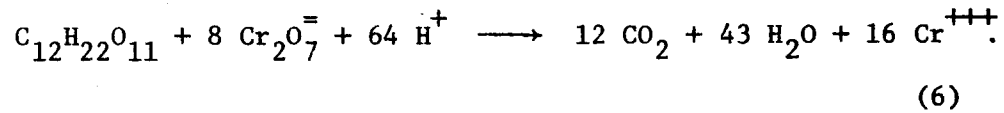
From equation 5, the TOD value is calculated to be:

$$TOD = \frac{1.12 \text{ grams of } O_2}{1 \text{ gram of } C_{12}H_{22}O_{11}}$$

COD is used often as a way to represent the oxygen demand of wastewater. The general equation for COD is



Upon substituting the values of a, b, and c for beet sugar factory condenser water effluent, the following equation is obtained.



From equation 6

$$\text{COD} = \frac{1.12 \text{ grams of } \text{O}_2}{1 \text{ gram of } \text{C}_{12}\text{H}_{22}\text{O}_{11}}$$

From the above expression, the ratio of COD to TOD is 1. The average COD to $\text{BOD}_{5\text{-day}, 20^\circ\text{C}}$ ratio is about 2.58, as shown in Table 6 and Figure 2, from experimental analysis in the laboratory.

This ratio may be somewhat unreliable as rather large variations in the ratios actually occurred, so one can not accurately predict BOD results from COD data.

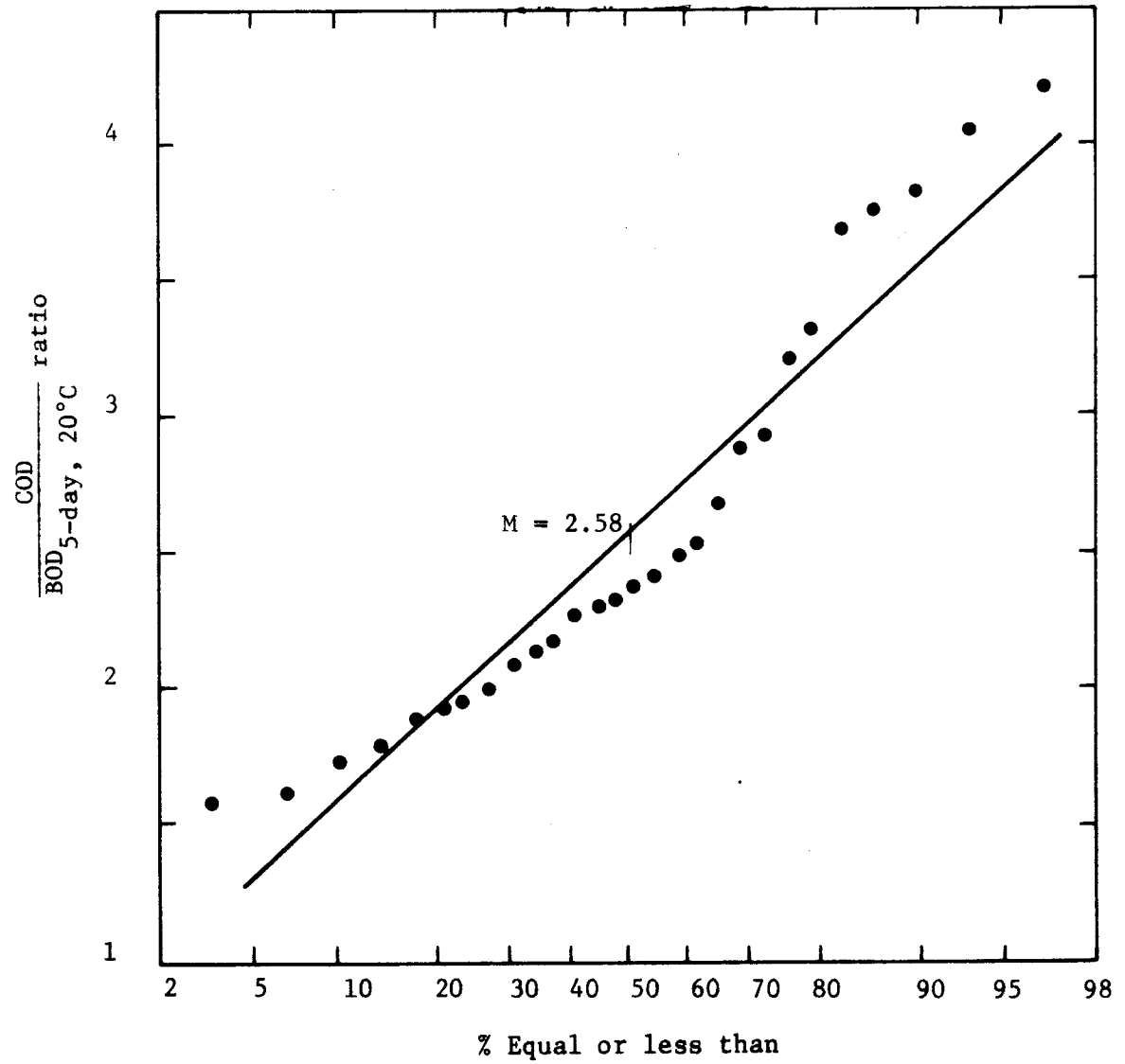
Table 6: Normal Frequency Analysis of $\frac{\text{COD}}{\text{BOD}_{5\text{-day}, 20^\circ\text{C}}}$ ratio

Order k	$\frac{\text{COD}}{\text{BOD}_{5\text{-day}, 20^\circ\text{C}}}$ X	$x = X - M$	x^2	$\frac{k}{n+1} 100\%$
1	1.58	-1	1	3.4
2	1.62	-0.96	0.92	6.9
3	1.73	-0.85	0.72	10.3
4	1.79	-0.79	0.62	13.8
5	1.87	-0.71	0.50	17.2
6	1.91	-0.67	0.45	20.7
7	1.94	-0.64	0.41	24.1
8	1.99	-0.59	0.35	27.6
9	2.08	-0.50	0.25	31.0
10	2.13	-0.45	0.20	34.5
11	2.16	-0.42	0.18	37.9
12	2.28	-0.30	0.09	41.4
13	2.30	-0.28	0.08	44.8
14	2.32	-0.26	0.07	48.3
15	2.36	-0.22	0.05	51.7
16	2.42	-0.16	0.03	55.2
17	2.49	-0.09	0.01	58.6
18	2.57	-0.01	0.00	62.1
19	2.72	0.14	0.02	65.5
20	2.88	0.30	0.09	69.0
21	2.92	0.34	0.12	72.4
22	3.20	0.62	0.38	75.9
23	3.35	0.77	0.59	79.3
24	3.67	1.09	1.12	82.8
25	3.75	1.17	1.37	86.2
26	3.82	1.24	1.54	89.7
27	4.05	1.47	2.16	93.1
28	4.21	1.63	2.66	96.6

$$M = \frac{\sum X}{n} = \frac{72.11}{28} = 2.58$$

$$\sigma = \sqrt{\frac{\sum x^2}{n-1}} = \sqrt{\frac{15.98}{28-1}} = 0.77$$

Figure 2: Probability plot of $\frac{\text{COD}}{\text{BOD}_{5\text{-day}, 20^\circ\text{C}}}$ ratio for condenser water effluent.



CHAPTER IV
EXPERIMENTAL EQUIPMENT AND PROCEDURES

Apparatus

Combined cooling and biotreatment of condenser water was accomplished in a small experimental system built and operated in the laboratory. The complete assembly was composed of the following three parts. (see Figure 3).

1. Heater: A constant temperature bath was used as a primary settling tank and as a reservoir for the maintenance of the inlet condenser water at constant temperature.
2. Reservoir: a vessel for collecting the outlet condenser water and for supplying the recirculating pump.
3. Packed column: a vertical cylinder serving as both a trickling filter and cooling tower. Three sections were combined in this transparent plastic column. In the upper part warm condenser water is distributed by a perforated plate to the middle part where PVC Raschig rings were randomly placed. The lower part serves as a catch basin for the cooled condenser water. The distributor plate was glued to the bottom of the upper section with an epoxy type glue and joined to the middle section by waterproof tape. A support plate was then glued to the bottom of the middle section and joined to the lower section by use of a rubber gasket. Stability of the column was insured by placing it in a steel frame.

The overflow weir in the heater permitted the suspended solids to settle to the bottom of the heater, thereby avoiding fouling or plugging the column.

Figure 3 is a schematic diagram of the apparatus. Further description is given in the following miscellaneous and in Tables 7 and 8.

Miscellaneous

1. Packing: PVC Raschig rings were chosen because of their high surface area, durability, chemical inertness to wastewater, high structural strength, and low pressure drop for air flow. Most of these properties are desirable for the packing in both a trickling filter and a cooling tower. The rings were cut from PVC pipe in such a manner that the length of each ring (0.84 inch) was equal to its outside diameter.
2. Distributor Plate: 16 one-eighth inch diameter holes were drilled evenly in the 6.4 inch diameter plastic plate. (0.25 inch thickness).
3. Support Plate: 20 one-half inch diameter holes were drilled evenly in the 6.4 inch diameter plastic plate. (0.25 inch thickness). The free area of the support plate is approximately 12 percent of the total area.
4. Air: Air from the laboratory compressed air source was passed into the column through a connection located below the support plate. Air flow rates were measured by a flowmeter (Fischer and Porter) located in the compressed air line to the column.
5. Temperature: Inlet and outlet temperatures of air and water were measured with thermometers located at the positions shown in Figure 3.

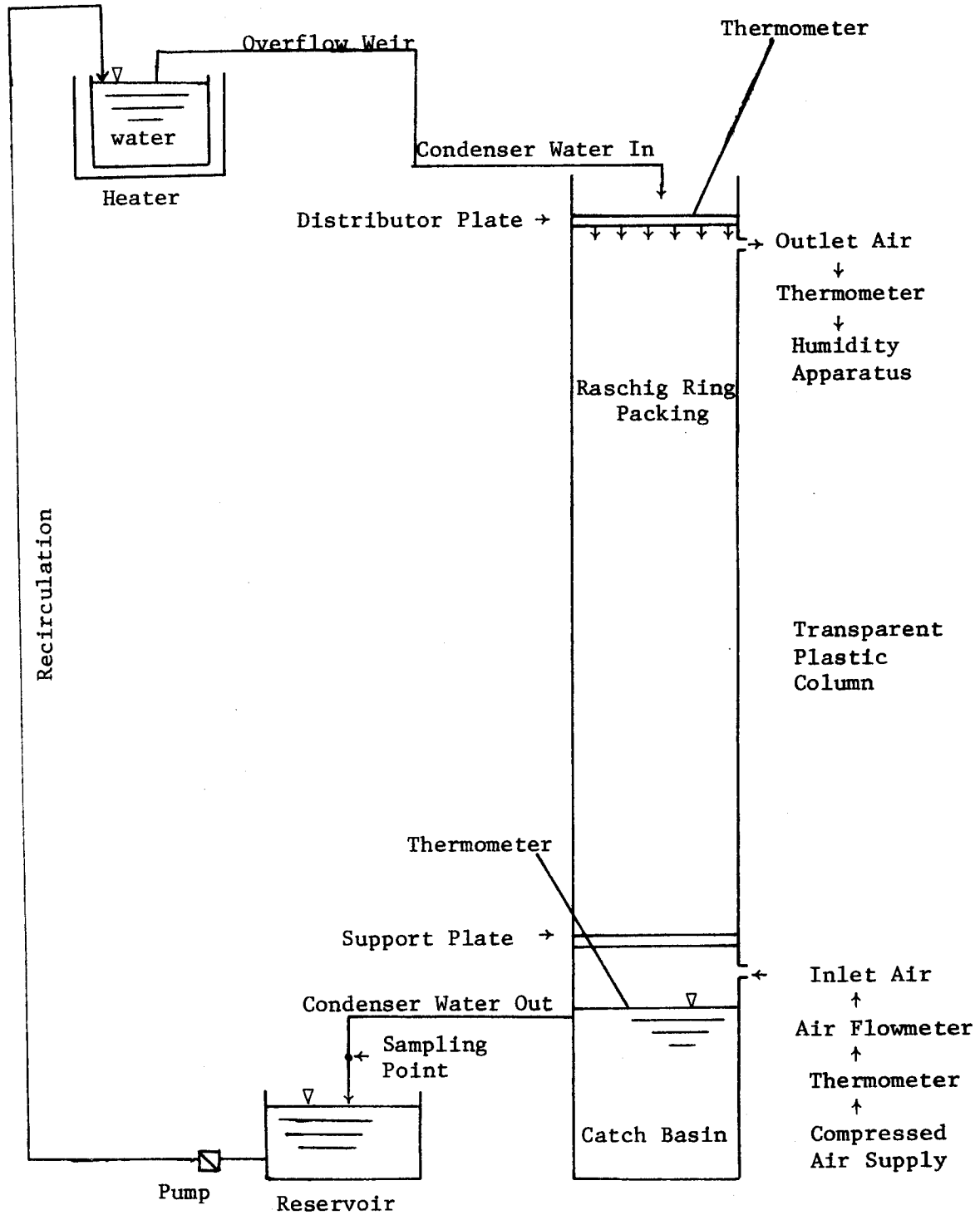


Figure 3: Schematic diagram of the apparatus.

Table 7: Dimensions of Experimental Apparatus

		Length (in.)	Width (in.)	Height (in.)	Outside Diameter (in.)	Inside Diameter (in.)	Cross-sectional Area (ft ²)	Volume (ft ³)
Heater		22.25	12.0	6.00			1.85	0.93
Reservoir		12.75	11.5	3.75			1.02	0.32
Plastic Column	upper			12.5	7.0	6.5	0.23	0.24
	middle			47.5	7.0	6.5	0.23	0.91
	lower			24.0	7.0	6.5	0.23	0.46

Table 8: Characteristics of PVC Raschig Rings

Nominal Size (in.)	Wall Thickness (in.)	Outside Diameter and Length (in.)	Approximate Number per ft ³	Approximate Dumped Weight per Volume Packing (lb/ft ³)	Price per Volume (\$/ft ³)	Surface Area per Unit Volume (ft ² /ft ³)	Porosity	Density (g/cm ³)	Thermal Conductivity $\frac{(\text{BTU})(\text{ft})}{(\text{hr})(\text{ft}^2)(^\circ\text{F})}$
0.84	0.08	0.84	2300	17.6	11.3	67.12	0.85	1.38	0.08

6. Humidity of Exit Air: The moisture content was measured by a humidity apparatus, (Baccarach's Hygrothermograph).

Operating Procedure

Condenser water effluent was obtained from the beet sugar factory and supplied to the heater and reservoir. The quantity of condenser water in the system was about 90 pounds. Regulation of temperature of inlet condenser water was controlled by adjusting the setting of the thermostat in the heater. The humidity of the inlet air was constant from the laboratory compressed air supply. Measurements of the temperature of inlet and outlet water and air, and the humidity of exit air were made at about 4-hour intervals. Valves for regulating air flow rate and liquid recirculation rate were adjusted about each 4-hour interval to give different flow rates. Because evaporation in such a high temperature process was significant, periodic addition of condenser water at 4-hour intervals was necessary to keep the amount of water constant in this closed system. Condenser water was used rather than distilled water in order to assure a constant food supply for the microorganisms.

In order to develop good bacterial growth in the column prior to actual testing, measurements of COD and inorganic nitrogen were delayed until the beginning of the third run of condenser water. Each run lasted about 10 days.

The measurements of COD (Potassium Dichromate method), ammonium nitrogen (Nessler's method), nitrate nitrogen (Cadmium reduction method), and nitrite nitrogen (1-Naphthylamine-Sulfanilic Acid method) were performed with the Hach colorimetric instrument.

CHAPTER V

RESULTS AND DISCUSSION

The experimental data show a water temperature decrease, usually about 30°F in one pass through the column, and a COD reduction of 31 to 84 percent for recirculation of 4 to 28 hours. More detailed information about COD and nitrogen removal, detention time, thermal considerations, and the microbiology study are presented in the following sections.

The heater serving as a primary settling tank had an accumulation of about 120 mg settleable matter per lb of condenser water per square foot of heater surface area per run. The catch basin at the bottom of the column removed large masses of biological growth which **had** been sloughed from the column packing, and also developed a thin layer of slime on its bottom surface. It was observed that a 12 percent free area on the support plate was adequate for free passage of water and air at the low flow rates used. Because an abundant supply of air was provided to the column at all times, oxidation of the adsorbed organic matter on the biological growth was not oxygen-limited. The slight decrease in pH of the water passing through the column was probably due to absorption of carbon dioxide formed by oxidation of carbon compounds present.

COD and Nitrogen Removal

The percent removal of COD and of nitrogen is shown in Tables 9 and 10, respectively. All data were based on average compositions of three samples.

Table 9: COD Removal

COD (mg/l) concentration		Temperature (°F)		Water flow rate (lb/hr)	Air/Water weight ratio **	Removal percent	Time between start and end (hr)	Operation passes ***
Start	End	Inlet	Outlet					
110	27.5	122	94	47.59	0.2087	84.4 [†]	28	14.8
100*	45	122	82	25.12	0.4433	56.6 ^{††}	4	1.1
110	55	122	94	47.59	0.2087	51.3 ^{††}	4	2.1
110	85	122	100	52.88	0.0014	31 ^{†††}	22.5	13.2

*Because the beet sugar factory was not in operation, the sample for this run was produced by adding sugar to tap water. Bacterial slime growth had been already established in the column.

**The ratio is based on the weight ratio, i.e., lb/hr of air to lb/hr of condenser water.

***The values in this column show the number of times that condenser water passes through the packed column during the run. Because biological action is very complex (i.e. biological action is not linear with respect to number of passages because of the decreasing concentration of adsorbable material), it is not practical to express removal in percent per pass. These values are calculated as follows:

$$\text{operation passes} = \frac{(\text{pumping water flow rate})(\text{time interval})}{(\text{total amount of water in the system})}$$

For example, if the pumping rate is 25.12 lb/hr, the measurement of COD is made after 4 hours, and the

Table 9 continued.

total water in the system is about 90 pounds, then from the above expression, the passes are 1.1.

[†]In order to keep the mass of condenser water in the system constant in the face of evaporation, 12 pounds of condenser water was added during the 28 hour operation. The removal percent was calculated as follows:

$$\# \text{ COD removed} = \# \text{ COD at start} + \# \text{ COD added} - \# \text{ COD at end}$$

There are two equations that might represent the percent removal of COD:

$$\% \text{ COD removal} = \frac{\# \text{ COD removed}}{\# \text{ COD at start}} = 1 + \frac{\# \text{ COD added} - \# \text{ COD at end}}{\# \text{ COD at start}} \quad (\text{see note at end of Table}) \quad (7)$$

$$\% \text{ COD removal} = \frac{\# \text{ COD removed}}{\# \text{ COD at start} + \# \text{ COD added}} = 1 - \frac{\# \text{ COD at end}}{\# \text{ COD at start} + \# \text{ COD added}} \quad (8)$$

The actual COD removal percent should be the average of the above equations 7 and 8,

Let c_0 = initial COD concentration in mg/l

c = final COD concentration in mg/l

w_0 = initial condenser water weight in pounds

Table 9 continued.

w = final condenser water weight in pounds

Δw = condenser water added in pounds .

Equations 7 and 8 can be written as follows:

$$\% \text{ COD removal} = 1 + \frac{c_o \Delta w - c w}{c_o w_o} \quad (9)$$

$$\% \text{ COD removal} = 1 - \frac{c w}{c_o (w_o + \Delta w)} \quad (10)$$

Substituting the following values into equations 9 and 10

$$c_o = 110 \text{ mg/ ,}$$

$$c = 27.5 \text{ mg/ ,}$$

$$w_o = 90 \text{ lbs,}$$

$$w = 85.2 \text{ lbs,}$$

$$\text{and } \Delta w = 12 \text{ lbs,}$$

values of 89.7% and 79.1% were obtained, respectively. So, COD removal was 84.4%.

Table 9 continued.

⁺⁺ There was no additional water added to the system because of the short time. In order to correct the COD removal percent because of the effect of evaporation, equations 9 and 10 were still used, and the same expression with $w = 0$ as follows:

$$\% \text{ COD removal} = 1 - \frac{cw}{c_o w_o}$$

Substituting $c = 45$, $c_o = 100$, $w = 86.8$, $w_o = 90$, and $c = 55$, $c_o = 110$, $w = 87.6$, and $w_o = 90$ for operation passes of 1.1 and 2.1, respectively, values of 56.6% and 51.3% removal were obtained, respectively.

35

⁺⁺⁺ Similarly substituting $c_o = 110$, $c = 85$, $w_o = 90$, $w = 87.4$, and $\Delta w = 6.4$ into equations 9 and 10, the COD removal was 31%.

Note: Equations 7 and 8 apply with adequate precision if pounds of COD added during the run are small compared to the amounts of COD originally present and left at the end of the run.

The data in Table 9 show that even with a low air flow rate ($G/L = 0.0014$) resulting in lower dissolved oxygen levels, COD removal is as high as 31 percent. It may also be noted that as the air/water ratio increases, the percent of COD removal increases also. When the air/water ratio is larger, either the detention time is longer, and/or higher dissolved oxygen concentration prevail. Although no studies were made on the rate of COD degradation, it is most probable that considerable time is required for this degradation to take place. Because the data shown in Table 9 are based on different fluid rates and different time intervals for COD measurement, it is difficult to determine the specific COD reduction rate.

If the rate of inflow is I , and the rate of recirculation is R , then the average number of passes, F' , is obtained as follows (28):

$$F' = 1 + \frac{R}{I} \quad (11)$$

Let F be the average number of effective passes, and $P = \% \text{ COD removal}$,

then, $\frac{P_1}{F_1} = \frac{P_2}{F_2} = \text{constant at the same air/water ratio.}$

If the removability of impurities is assumed to decrease as the number of passes is multiplied, a weighting factor, f , can be introduced into equation 11 to obtain a satisfactory expression for the average number of effective passes, F , of the putrescible matter through the treatment unit. Equation 11 becomes (29)

$$F = \frac{F'}{[1 + (1 - f)(R/I)]^2} \quad (12)$$

One can express equation 12 as follows:

$$\frac{F_2}{F_1} = \frac{F'_2/F'_1}{[I + (1 - f)(R/I)_2]^2 / [I + (1 - f)(R/I)_1]^2}$$

With some algebra, the following expression is obtained:

$$(1 - f) = \frac{\sqrt{\frac{F'_2 F_1}{F'_1 F_2}} - 1}{(R/I)_2 - (R/I)_1 \sqrt{\frac{F'_2 F_1}{F'_1 F_2}}}$$

Substituting $P_2/P_1 = 51.3/84.4 = 0.608$, $F'_2/F'_1 = 2.1/14.8 = 0.142$, $(R/I)_1 = 14.8 - 1 = 13.8$, and $(R/I)_2 = 2.1 - 1 = 1.1$, into the above expression, the weighting factor, f , is found to be 0.907.

If F is the dependent variable, and if f is constant, F reaches a maximum value (29) at

$$R/I = (2f - 1)/(1 - f) = 8.78.$$

Then, the maximum F , from equation 12 is 2.97.

The F values in Table 10 were calculated from equation 12 with the known F' , R/I , and f , and the maximum value of F is also shown for comparison.

The relationship between P/F and water flow rate multiplied by COD concentration is shown in Figure 4.

Ordinarily the percent BOD removal by this kind of biological purification would be expected to be somewhat higher than the percent COD removal.

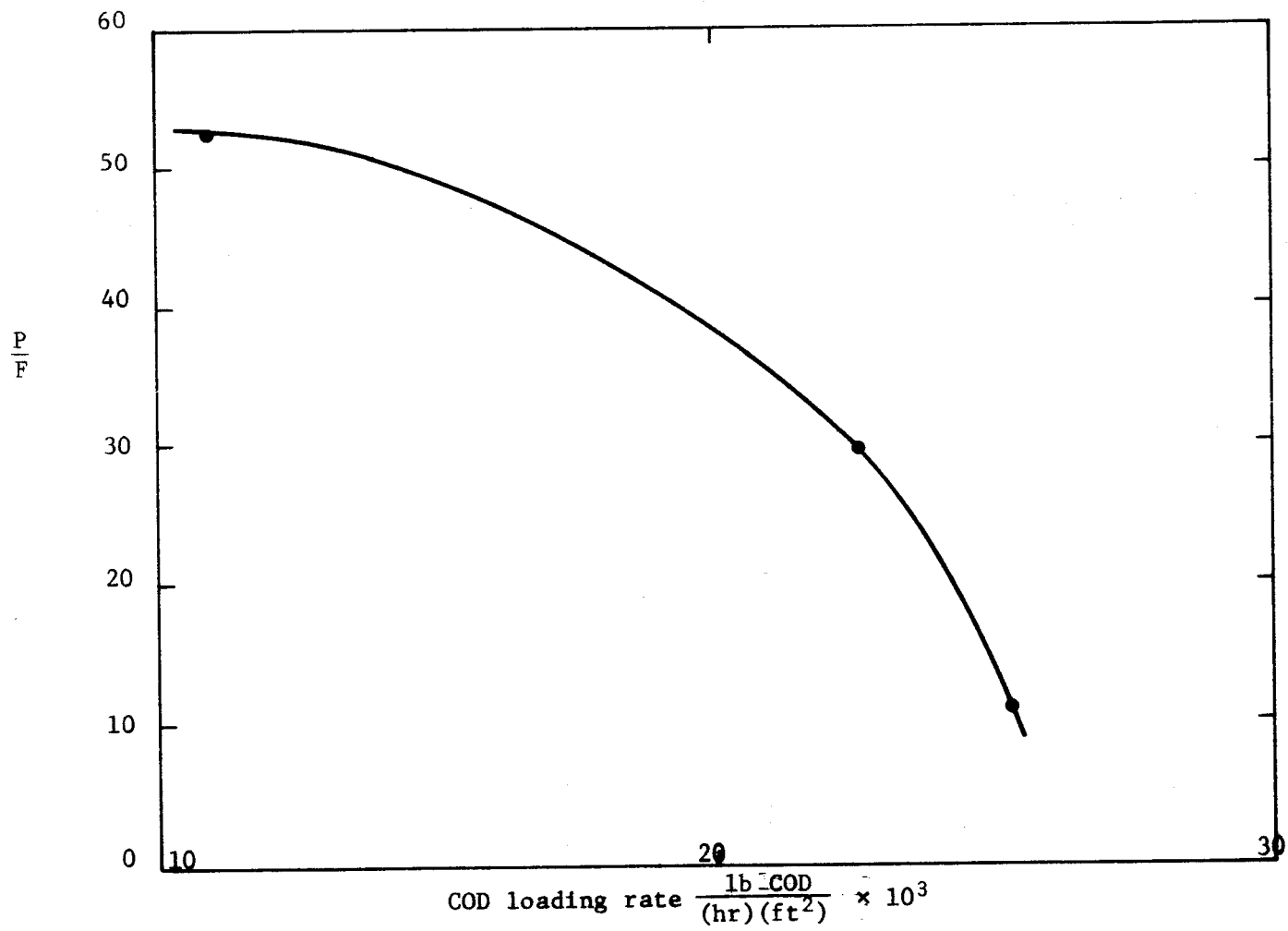


Figure 4: Relationship between % COD removal per effective pass (P/F) and COD loading rate.

Table 10: % COD Removal per Effective Pass

(Water velocity)(COD) lb COD/(hr)(ft ²) × 10 ³	F'	R/I	F	% COD removal (P)	P/F
22.8	14.8	13.8	2.85	84.4	29.6
10.9	1.1	0.1	1.08	56.6	52.4
22.8	2.1	1.1	1.73	51.3	29.6
25.3	13.2	12.2	2.90	31	10.7
		*8.78	*2.97		

*F has a maximum value of 2.97 at (R/I) = 8.78.

The data in Table 11 indicate that most of the NH₃ removal is by air stripping rather than by oxidation to nitrite nitrogen. For example, for the 0.6 G/L weight ratio run, of the 9 mg/l of NH₃ removal, only about 1 mg/l was oxidized to nitrite and then to nitrate, and the rest was due to air stripping.

The weighting factor, *f*, is calculated to be 0.61 and 0.75, respectively, for the air-water weight ratio of 0.3 and 0.6, respectively, in the ammonia-nitrogen removal data.

Because the data for nitrogen removal in Table 11 were obtained from a synthetic working medium instead of condenser water effluent from the beet sugar factory, the results show only the ability of air stripping to remove nitrogen in the synthetic medium without giving a quantitative correlation with the beet sugar factory condenser water effluent.

Because most of the nitrogen in condenser water exists in the form of ammonia (introduced by evaporating and cooling operations), the

Table 11*: Nitrogen Removal

	Start mg/ℓ	End mg/ℓ		Removal percent		G/L Weight Ratio
		1 hour interval (0.26 passes)	24 hour interval (6.20 passes)	1 hour interval (0.26 passes)	24 hour interval (6.20 passes)	
Ammonia-Nitrogen	16	15.5	12	3	25	0.3
Ammonia-Nitrogen	18	15	9	17	50	0.6
Nitrate-Nitrogen	2	2	2.5	0	-25	0.3
Nitrate-Nitrogen	2	2	3	0	-50	0.6
Nitrite-Nitrogen	0.25	0.24	0.2	4	20	0.3
Nitrite-Nitrogen	0.25	0.24	0.2	0	20	0.6
Total Nitrogen	18.25	17.74	14.7	3	19	0.3
Total Nitrogen	20.25	17.25	12.2	15	40	0.6

*Because the beet sugar factory was not in operation, synthetic samples were made by adding NH_4Cl , NaNO_3 , and NaNO_2 to provide ammonia-nitrogen, nitrate-nitrogen and nitrite-nitrogen, respectively. Bacterial slime growth had been already established in the column. Operation pass was defined earlier.

removal of nitrogen centers on the removal of ammonia-nitrogen. Hence it appears that nitrogen removal from actual condenser water effluent should be effective when air is used as the stripping medium.

Detention Time

Detention time or contact time in the column, an important variable in the biological treatment system, was measured with the dye, Rhodamine WT. The dye was added as the water passed through the distributor plate. The concentration of the dye was measured in a Fluorometer (Model 111, G.K. Turner Association, Palo Alto, California). Because fluorescence varies linearly with concentration below several hundred parts per billion, it follows that the fluorometer dial readings vary linearly with concentration. The curve of time vs. fluorometer dial reading is given in Figure 5.

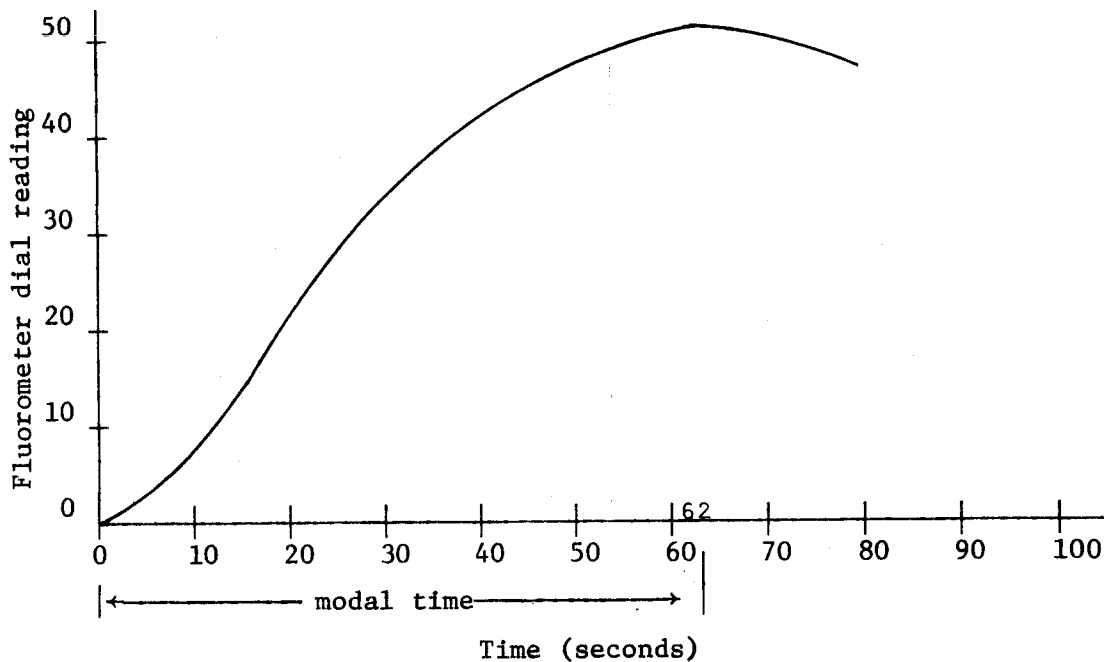


Figure 5: Fluorometer dial reading-time curve for sudden dump.

In this case tap water was used instead of condenser water from the beet sugar factory, because the factory was closed. Moreover, a large part of the biological growth had been removed for microbiology studies. Therefore, the data for detention time are only for reference.

In order to collect outlet water as quickly as possible, the catch basin shown in Figure 3 was removed, and replaced by another plate which allowed water to pass through a single central hole. The detention time calculated is modal time (i.e. time at which the maximum dye concentration and/or maximum fluorometer dial reading was observed), and lies between 60 and 250 seconds when the ratio of air to water ranges from 0.1 to 0.75. At a constant water flow rate, the detention time increased as the air flow rate increased because of liquid hold-up by air friction. The data for detention time with various fluid flow rates are shown in Table 12.

Howland (30) stated that the detention time of wastewater within a trickling filter was related to the filter depth, the hydraulic loading, the nature of the packing, and the water viscosity. He suggested the following relationship obtained from a derivation based on a flowing liquid film on an inclined plane:

$$t_d = c h \left(\frac{\nu}{g} \right)^{1/3} \left(\frac{A/V}{Q} \right)^{2/3} \quad (13)$$

where

t_d = detention time, seconds

h = filter depth, ft

ν = kinematic viscosity of the wastewater, ft²/sec.

g = acceleration of gravity, 32.2 ft/sec².

Table 12: Detention Time

Air Flow Rate G' (Lb/hr)	Water Flow Rate L' (Lb/hr)	G/L	Modal Detention Time t (seconds)
6.187	29.080	0.213	115
	60.657	0.102	62
	47.592	0.130	76
	30.935	0.200	108
	15.232	0.406	205
7.424	29.080	0.255	135
	48.230	0.154	90
	30.800	0.241	136
	22.542	0.329	170
	15.060	0.495	225
8.662	29.000	0.299	160
	52.237	0.166	90
	31.498	0.275	146
	24.749	0.350	177
	15.000	0.577	240
9.899	29.000	0.341	170
	58.230	0.170	94
	31.425	0.315	165
	17.280	0.573	234
11.137	29.000	0.384	187
	30.936	0.360	185
	21.543	0.517	235
	14.750	0.755	255
0	11.898	0.000	60
	16.393	0.000	50
	23.567	0.000	42
	28.555	0.000	36
	34.372	0.000	32
	43.626	0.000	26
	44.419	0.000	27

Q = volume/(unit area)(unit time), ft/sec.

A/V = surface area/unit volume of bed, ft^{-1}

c = a dimensionless constant that reflects film buildup.

It can be shown that

$$c = K k^{1/3} \quad (14)$$

where

K is the fraction of the pore volume occupied by the liquid,
dimensionless

k = dimensionless coefficient = 5 (31).

Substituting the following constants into equation 13,

h = 3.958 ft

v = 1.0863×10^{-5} ft^2/sec at 20°C

g = 32.2 ft/sec^2

A/V = 67.12 ft^2/ft^3

equation 13 simply becomes

$$t_d = c(2.11)(1/Q)^{2/3} \quad (15)$$

With the data in Table 12 at an air flow rate of zero, the plot of detention time, t_d (sec), vs. water flow rate, Q (ft/sec), on log-paper in Figure 6 yields a straight line. Compared with Howland's equation, the slope in Figure 6 is apparently the same which means that the detention time is inversely proportional to the water flow rate to the 2/3 power. The intercept in Figure 6 is 0.24 (calculated by substituting $t_d = 24$, $Q = 10^{-3}$ into equation 15), which gives c in equation 15 a value of 0.1137. From equation 14, the fraction of the pore volume occupied by the liquid, K , is about 0.0665.

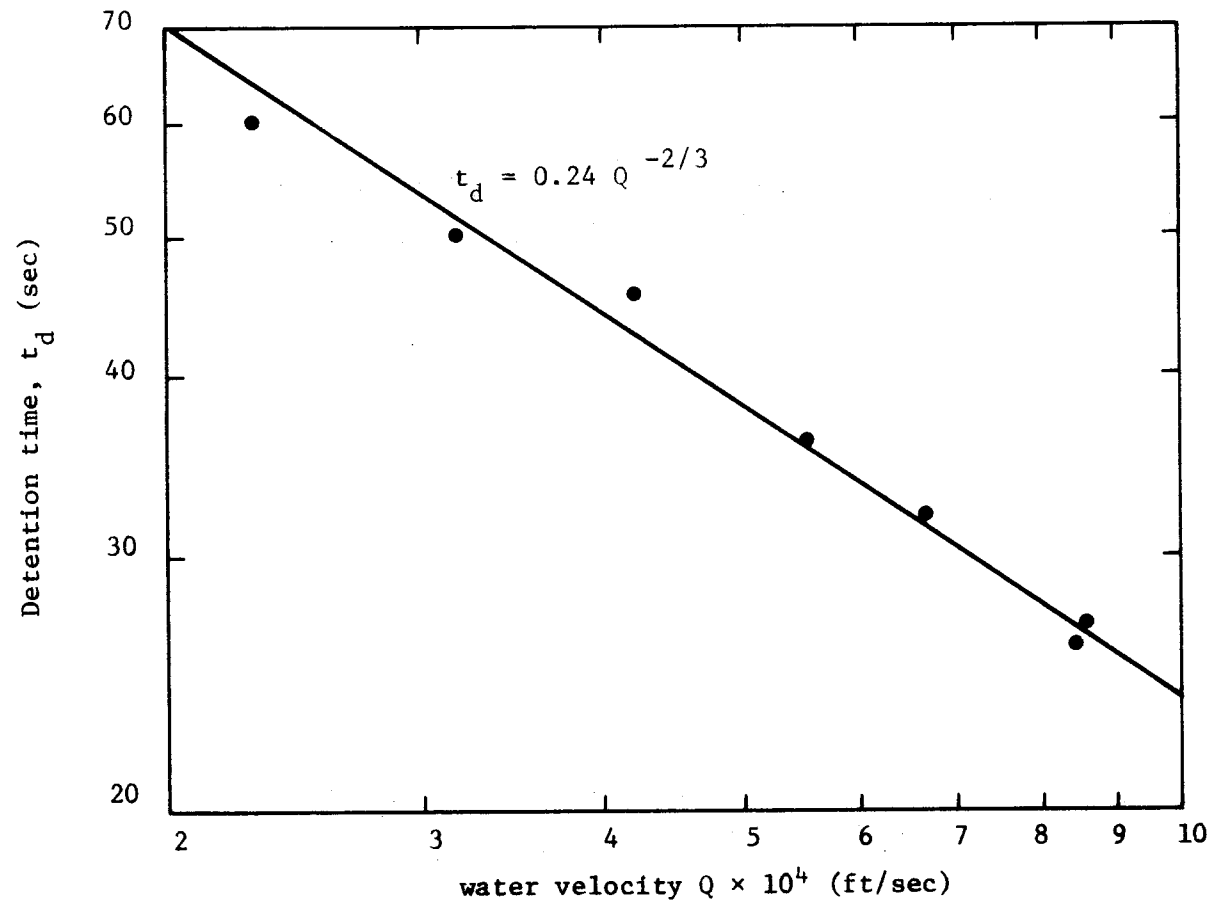


Figure 6: Relation between application rate and detention time with zero air flow rate.

Obviously equation 13 strictly applies at an air flow rate of zero. Air flowing counter-current to the downward liquid flow will increase the detention time in the column. Designating this increase in detention time by Δt , then the total detention time, t , is:

$$t = t_d + \Delta t . \quad (16)$$

The increase in detention time caused by the effect of the air flow, Δt , can be determined from equation 16 using observed values of t and calculated values of t_d (using Figure 6). The plot of Δt vs. G/L ratio yields a straight line passing through the origin as shown in Figure 7. The equation in Figure 7 is:

$$\Delta t = 400 (G/L) . \quad (17)$$

It is observed from Figure 7 that when the G/L ratio exceeds about 0.4, a linear relationship no longer exists.

In conclusion, the following semi-empirical equation can be obtained when the G/L ratio is less than about 0.4,

$$t = 0.1137 \text{ h} \left(\frac{v}{g} \right)^{1/3} \left(\frac{A/V}{Q} \right)^{2/3} + 400 (G/L) . \quad (18)$$

Thermal Considerations

The average temperature of the condenser water entering and leaving the packed column was 121°F and 81°F, respectively. A temperature drop of at least 30°F could be maintained during the experiment when the air-water weight ratio was greater than 0.1. The detailed data are tabulated in Table 13.

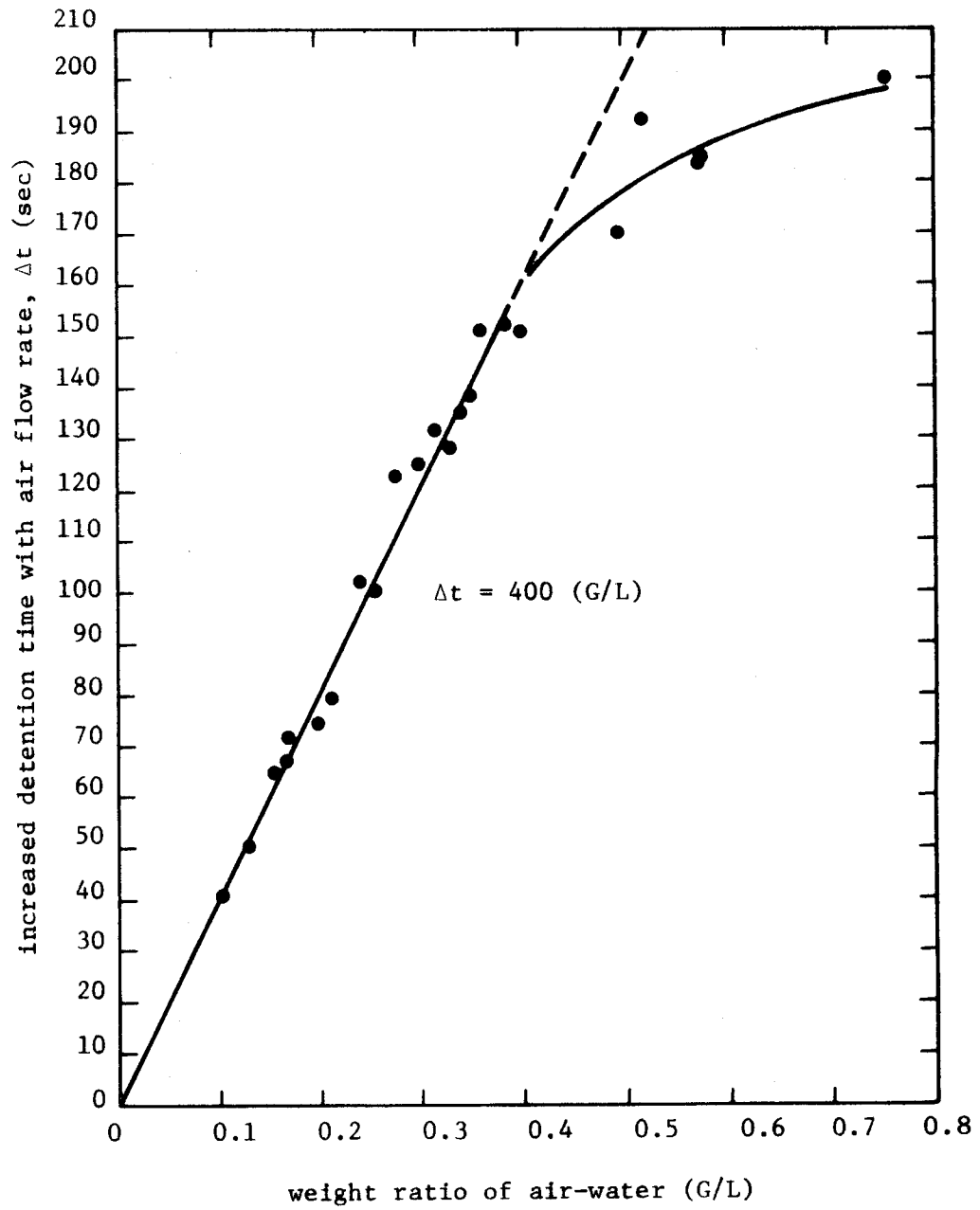


Figure 7: Relationship between weight rate ratio of air-water to increased detention time, Δt .

Description of the calculation of cooling
performance in Table 13

The following values are constants through the whole calculations

- (1) dry-bulb temperature of entrance air = 71°F
- (2) wet-bulb temperature of entrance air = 51°F. The wet bulb temperature was measured with a thermometer which was covered by a wick, which was saturated with pure water and immersed in a stream of air (psychrometer).
- (3) humidity of entrance air = 0.005 lb of water /lb of dry air, calculated from dry-bulb and wet-bulb temperatures and psychrometric chart, corrected to an atmospheric pressure of 24.92 inches of mercury.
- (4) humid heat of entrance air = 0.2423 BTU/(lb of dry air)(°F), calculated from the following equation

$$c_s = (c_p)_{\text{air}} + (c_p)_{\text{water vapor}} H = 0.24 + 0.45 H$$

for water vapor temperatures between 50 and 250°F and air temperatures between 32 and 100°F

- (5) enthalpy of entrance air = 14.83 BTU/lb, calculated from the following equation

$$i = H \lambda_o + c_s (T - T_o)$$

where $T_o = 32^\circ\text{F}$, $T = 71^\circ\text{F}$, and $\lambda_o = 1075.8 \text{ BTU/lb}$

- (6) cross-sectional area of column = 0.23 ft²
- (7) surface area/unit volume = 67.12 ft²/ft³
- (8) height of column (Z) = 3.96 feet.

Description of the calculations of cooling performance in Table 13 is as follows:

- column (1): time between measurements
- (2): measured
- (3): measured
- (4): measured
- (5): from columns (4) and (6) and psychrometric chart, corrected to an atmospheric pressure of 24.92 inches of mercury
- (6): measured with a humidity apparatus (Baccarach's Hygrothermograph)
- (7): measured in the line of inlet water
- (8): measured with an air flowmeter.
- (9): column (8)/column (7)
- (10): from columns (4) and (6) and psychrometric chart, corrected to an atmospheric pressure of 24.92 inches of mercury
- (11): from column (10) and equation $c_s = 0.24 + 0.45 H$
- (12): from column (2) and the steam tables
- (13): from column (3) and the steam tables
- (14): from columns (4) and (10) and (11) and equation
- $$i = H \lambda_o + c_s (T - T_o)$$
- (15): column (7) × column (12) multiplied by 0.23 ft² (horizontal cross-sectional area of column)
- (16): column (8) × 14.83 BTU/lb (enthalpy of entrance air) and multiplied by 0.23 ft²
- (17): column (15) + column (16)
- (18): column (7) × column (13) multiplied by 0.23 ft²
- (19): column (8) × column (14) multiplied by 0.23 ft²

Table 13: Cooling Performance

Time time = 0 at start of run	Temperatures				Relative humidity in exit air	Flow Rates		Weight ratio of air to water	Humidity of exit air
	water		exit air			water	air		
	in	out	dry-bulb	wet-bulb		(7)	(8)		
(1)	(2)	(3)	(4)	(5)	(6)	(7)	(8)	(9)	(10)
hours	(°F)	(°F)	(°F)	(°F)	H _R (%)	L $\left(\frac{\text{lb}}{(\text{hr})(\text{ft}^2)} \right)$	G $\left(\frac{\text{lb}}{(\text{hr})(\text{ft}^2)} \right)$	G/L	H $\left(\frac{\text{lb of water}}{\text{lb of dry air}} \right)$
0	118	86	102	91	70	74.74	21.52	0.288	0.0380
7 1/4	118	78.8	102	91	68	65.52	21.52	0.328	0.0380
12 3/4	118	77	100	87.8	69	52.87	21.52	0.407	0.0351
10 1/2	116	84	101	91	72	86.22	21.52	0.250	0.0379
15	122	90	103	91.5	70	86.22	21.52	0.250	0.0392
2	121	95	108	101	82	149.43	37.66	0.252	0.0544
7 1/2	118	80.6	107	100.8	83	103.48	37.66	0.364	0.0534
15	120	84	106	99.5	82	114.96	37.66	0.328	0.0511
4	124	81.2	112	103.3	78	122.61	48.43	0.395	0.0584
5 1/2	122	80.6	108	99.5	78	114.96	48.43	0.421	0.0515
2 1/2	124	76.8	107	95.8	72	97.74	48.43	0.495	0.0458
6	122	78.8	106	95.1	72	103.48	48.43	0.468	0.0444
5	122	78.8	104	93.2	72	91.96	48.43	0.527	0.0417
11 5/6	122	82.4	108	97.3	73	114.96	48.43	0.421	0.0480
3 2/3	122	78.8	105	94	72	94.83	48.43	0.511	0.0430
6	122	85.1	110	99.2	73	106.35	32.26	0.303	0.0511
14 1/2	122	81.5	107	100.1	82	90.83	32.26	0.355	0.0527
2 1/2	121.6	81.3	108	102.7	86	89.09	32.26	0.362	0.0573
5	121	79.7	108	101.6	83	82.17	32.26	0.393	0.0551
5	121.8	78.8	106	98.9	81	74.74	32.26	0.432	0.0504
3 1/3	122	77	105	97.2	80	71.26	37.66	0.528	0.0482
8 3/4	122	75.2	105	96.2	77	66.70	37.66	0.565	0.0462
3 3/4	120	75.2	104	96.5	80	65.52	43.04	0.657	0.0467
3 1/4	121	73.8	105	97.4	79	65.52	43.04	0.657	0.0475
3 3/4	121	73.4	103	94.4	77	64.96	43.04	0.663	0.0434

(Table 13 continued)

Humid heat of exit air	Enthalpy			Heat in			Heat out			Net heat loss through column walls	Humidity difference
	water		exit air	water	air	total	water	air	total		
	in	out									
(11)	(12)	(13)	(14)	(15)	(16)	(17)	(18)	(19)	(20)	(21)	(22)
$c_p \left[\frac{\text{BTU}}{(\text{lb of dry air})(^\circ\text{F})} \right]$	i (BTU/lb)			BTU/hr			BTU/hr			BTU/hr	$\Delta H \left(\frac{\text{lb water vapor}}{\text{lb dry air}} \right)$
0.2571	85.92	54.00	58.88	1477	73	1550	928	292	1220	330	0.0330
0.2571	85.92	46.82	59.14	1295	73	1368	706	293	999	369	0.0330
0.2558	85.92	45.02	55.16	1045	73	1118	548	273	821	297	0.0301
0.2571	83.93	52.01	58.51	1664	73	1737	1031	290	1321	416	0.0329
0.2576	89.92	57.99	60.46	1783	73	1856	1150	299	1449	407	0.0342
0.2645	88.92	62.98	78.63	3056	128	3184	2165	681	2846	338	0.0494
0.2640	85.92	48.62	77.25	2045	128	2173	1157	669	1826	347	0.0484
0.2630	87.92	52.01	74.44	2325	128	2453	1375	645	2020	433	0.0461
0.2663	91.91	49.22	84.13	2592	165	2757	1388	937	2325	432	0.0534
0.2632	89.92	48.62	75.41	2377	165	2542	1286	840	2126	416	0.0465
0.2606	91.91	44.83	68.82	2066	165	2231	1008	767	1775	456	0.0408
0.2600	89.92	46.82	67.01	2140	165	2305	1114	747	1861	444	0.0394
0.2588	89.92	46.82	63.50	1902	165	2067	990	708	1698	369	0.0367
0.2616	89.92	50.41	71.52	2377	165	2542	1333	797	2130	412	0.0430
0.2594	89.92	46.82	65.20	1961	165	2126	1021	726	1747	379	0.0380
0.2630	89.92	53.10	75.49	2199	110	2309	1299	560	1859	450	0.0461
0.2637	89.92	49.52	76.47	1878	110	1988	1035	567	1602	386	0.0477
0.2658	88.42	49.32	81.84	1812	110	1922	1011	607	1618	304	0.0523
0.2630	88.92	47.92	79.27	1681	110	1791	906	588	1494	297	0.0501
0.2627	89.72	46.32	73.66	1542	110	1652	805	547	1352	300	0.0454
0.2617	89.92	45.02	70.96	1474	128	1602	738	615	1353	249	0.0432
0.2608	89.92	43.23	68.74	1379	128	1507	663	595	1258	249	0.0412
0.2610	87.92	43.23	69.03	1325	147	1472	652	683	1335	137	0.0417
0.2614	88.92	41.83	70.18	1340	147	1487	630	695	1325	162	0.0425
0.2595	88.92	41.43	65.11	1328	147	1475	619	645	1264	211	0.0384

(Table 13 continued)

Calculated evaporation from column	Added water	Calculated evaporation from reservoir and heater	Calculated $K_y a$	Heat out in water assuming all heat loss through walls remained in water	Enthalpy of outlet water if heat loss remained in water	Temperature of outlet water if heat loss remained in water	Average temperature between actual outlet water and condition in column (29)
(23)	(24)	(25)	(26)	(27)	(28)	(29)	(30)
lb of water/hr	$\frac{\text{lb of water}}{\text{hour}}$	lb of water/hr	$\frac{\text{lb}}{(\text{hr})(\text{ft}^3)(\Delta H)}$	BTU/hr	BTU/lb	$^{\circ}\text{F}$	$^{\circ}\text{F}$
0.163	0.560	0.397	5.62	1258	73.18	105.2	95.6
0.163	0.541	0.378	6.99	1075	71.33	103.4	91.1
0.149	0.513	0.364	6.55	845	69.49	101.5	89.3
0.163	0.564	0.401	6.19	1447	72.97	104.0	94.0
0.169	0.572	0.403	4.80	1557	78.52	110.6	100.3
0.428	0.878	0.450	12.48	2503	72.83	104.9	100.0
0.419	0.941	0.522	20.37	1504	63.19	95.2	87.9
0.399	0.781	0.382	14.49	1808	68.38	100.4	92.2
0.595	1.075	0.480	25.65	1820	64.54	96.6	88.9
0.518	1.054	0.536	22.35	1702	64.37	96.4	88.5
0.455	0.855	0.400	19.52	1464	65.12	97.2	87.0
0.439	0.929	0.490	18.42	1558	65.46	97.5	88.2
0.401	0.823	0.422	20.49	1359	64.26	96.3	87.6
0.479	0.945	0.466	18.56	1745	70.00	102.0	92.2
0.423	0.852	0.429	21.32	1400	65.19	96.2	87.5
0.342	0.850	0.508	12.81	1749	71.50	103.5	94.3
0.354	0.755	0.401	14.72	1421	68.02	100.0	90.8
0.388	0.793	0.405	15.89	1315	64.18	96.2	88.8
0.372	0.715	0.343	15.91	1203	63.65	95.7	87.7
0.337	0.698	0.361	14.91	1105	64.28	96.3	87.6
0.374	0.880	0.506	17.02	987	60.22	92.2	84.6
0.357	0.794	0.437	17.08	912	59.45	91.5	83.4
0.413	0.663	0.250	20.81	789	52.36	84.3	79.8
0.421	0.657	0.236	22.24	792	52.55	84.5	79.2
0.380	0.833	0.453	19.16	830	55.56	87.6	80.5

(Table 13 continued)

Heat out in air assuming all heat loss remained in air	Enthalpy of exit air if heat loss remained in air	Average air enthalpy between actual exit air and condition in column (32)	Adjusted $K_y a$	L G	L/G	α	Mass transfer film coefficient, gas phase
(31)	(32)	(33)	(34)	(35)	(36)	(37)	(38)
BTU/hr	BTU/lb	BTU/lb	$\frac{\text{lb}}{(\text{hr})(\text{ft}^2)(\Delta H)}$	$\left[\frac{\text{lb}}{(\text{hr})(\text{ft}^2)}\right]^2$			$K_y \cdot \frac{\text{lb}}{(\text{hr})(\text{ft}^2)(\Delta H)}$
622	125.66	92.3	11.16	1608	3.47	0.0177	0.166
662	133.74	96.4	14.51	1410	3.05	0.0245	0.216
570	115.15	85.2	11.03	1138	2.46	0.0271	0.164
706	142.67	100.6	13.51	1856	4.01	0.0175	0.201
706	142.67	101.6	10.49	1856	4.01	0.0136	0.156
1019	117.67	98.2	17.72	5628	3.97	0.0148	0.264
1016	117.32	97.3	29.23	3897	2.75	0.0322	0.435
1078	124.48	99.5	24.20	4329	3.05	0.0211	0.361
1369	122.89	103.5	32.82	5938	2.53	0.0292	0.489
1256	112.75	94.1	27.69	5568	2.37	0.0267	0.413
1223	109.78	89.3	23.69	4734	2.02	0.0265	0.353
1191	106.91	87.0	23.39	5010	2.14	0.0240	0.348
1077	96.68	80.1	25.60	4454	1.90	0.0294	0.372
1209	108.53	90.0	22.08	5568	2.37	0.0222	0.329
1105	99.19	82.2	25.50	4593	1.96	0.0297	0.380
1010	136.12	105.8	20.76	3431	3.30	0.0224	0.309
953	128.44	102.5	21.25	2930	2.82	0.0291	0.317
911	122.78	102.3	25.67	2874	2.76	0.0319	0.382
885	119.27	99.3	22.85	2651	2.55	0.0340	0.340
847	114.15	93.9	19.05	2411	2.32	0.0343	0.284
864	99.77	84.4	19.46	2684	1.89	0.0364	0.290
844	97.46	83.1	19.03	2512	1.77	0.0380	0.284
820	82.83	75.9	21.56	2820	1.52	0.0424	0.321
857	86.57	78.4	22.77	2820	1.52	0.0453	0.339
856	86.46	75.8	20.35	2796	1.51	0.0392	0.303

column

- (20): column (18) + column (19)
- (21): column (17) - column (20)
- (22): column (10) - 0.005 (humidity of entrance air)
- (23): column (8) × column (22) multiplied by 0.23 ft²
- (24): measured, the quantity of water added to keep water level constant during each run, divided by time interval
- (25): column (24) - column (23)
- (26): calculated from equation 19 and Figures 8 and 9, with the data in columns (2), (3), (8), (14), and 14.83 BTU/lb (enthalpy of air in)
- (27): column (18) + column (21)
- (28): column (27)/[column (7) times 0.23 ft²]
- (29): from column (28) and the steam tables
- (30): average of column (3) and column (29)
- (31): column (19) + column (21)
- (32): column (31)/[column (8) times 0.23 ft²]
- (33): average of column (14) and column (32)
- (34): calculated with the data in columns (2), (8), (30), (33), and 14.83 BTU/lb (enthalpy of entrance air)
- (35): column (7) × column (8)
- (36): column (7)/column (8)
- (37): calculated, using equation 24, and columns (26) and (35)
- (38): column (34)/67.12 where 67.12 is surface area per unit volume.

From Table 13, it is observed that the heat loss from the column and the amount of evaporation in the heater and reservoir are significant. The heat loss is mainly due to heat transfer through the walls of the column during operation. The exposed water surface in the reservoirs contributes to the total evaporation. Evaporation in the column itself should increase as the air flow rate increases if the water flow rate remains constant. Likewise, evaporation should increase as the water flow rate increases if the air flow rate remains constant, because the packing is not completely wet at low water flow rates. [According to Morris and Jackson (32), the water rate should be more than 3,000 lb/(hr)(ft²) before the column will be completely wet]. No definite relationship between evaporation rate and an increased air-water weight ratio can be observed from the experimental data.

The mass transfer coefficient ($K_Y a$) has been calculated from the following equation (33):

$$K_Y a = \frac{G}{Z} \int_{i_1}^{i_2} \frac{di}{i^* - i} \quad (19)$$

where

$K_Y a$ is the overall volumetric mass transfer coefficient,
lb/(hr)(ft³)(ΔH)

G is superficial mass velocity of dry air, lb/(hr)(ft²)

K_Y is mass transfer film coefficient, gas phase, lb/(hr)(ft²)(ΔH)

a is the air-water contact surface area per unit volume of bed,
ft²/ft³.

Z is the height of apparatus, ft

i is the air enthalpy, BTU/lb of dry air
 i^* is the enthalpy of a saturated air-water mixture in equilibrium with the bulk of the water, BTU/lb of dry air, and the subscripts 1 and 2 denote the bottom and the top of the cooling tower, respectively.

In order to plot the equilibrium curve shown in Figure 8, the following equation was used. This equilibrium curve is plotted as the enthalpy of saturated air at various temperatures.

$$i^* = (0.24 + 0.45 H^*)(T_L - 32) + 1075.8 H^* \quad (20)$$

where

T_L is water temperature, °F

$$H^* = \frac{18}{29} \frac{\bar{p}}{(p - \bar{p})} \quad \text{and}$$

\bar{p} is the vapor pressure of water at temperature T_L , inches of mercury,

p is the atmospheric pressure which is near 24.92 inches of mercury on the third floor of the Engineering Research Center, Colorado State University, Fort Collins, Colorado (Elevation above mean sea level is 5,000 feet).

The actual operating line shown in Figure 8 was obtained from the data of the first row in Table 13. It connects the terminal conditions for water temperature with respect to the enthalpy of the water vapor-air mixture. Now with the data in Figure 8, an equilibrium curve indicating i^* and operating line indicating i , Figure 9 is obtained by plotting $1/i^* - i$ vs i . The area under the curve in Figure 9 was measured with a

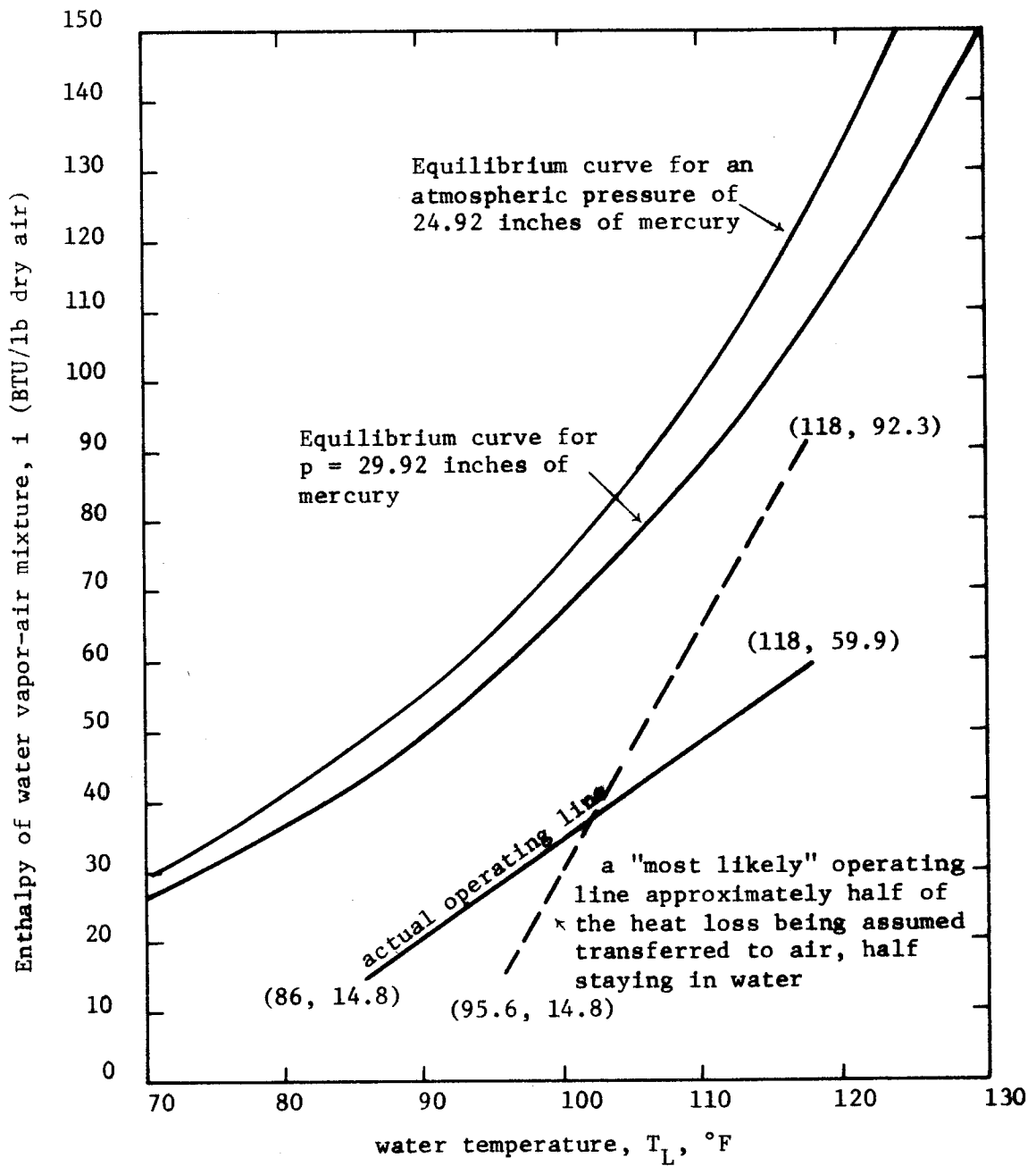


Figure 8: Equilibrium and operating curves used in the solution of equation 19.

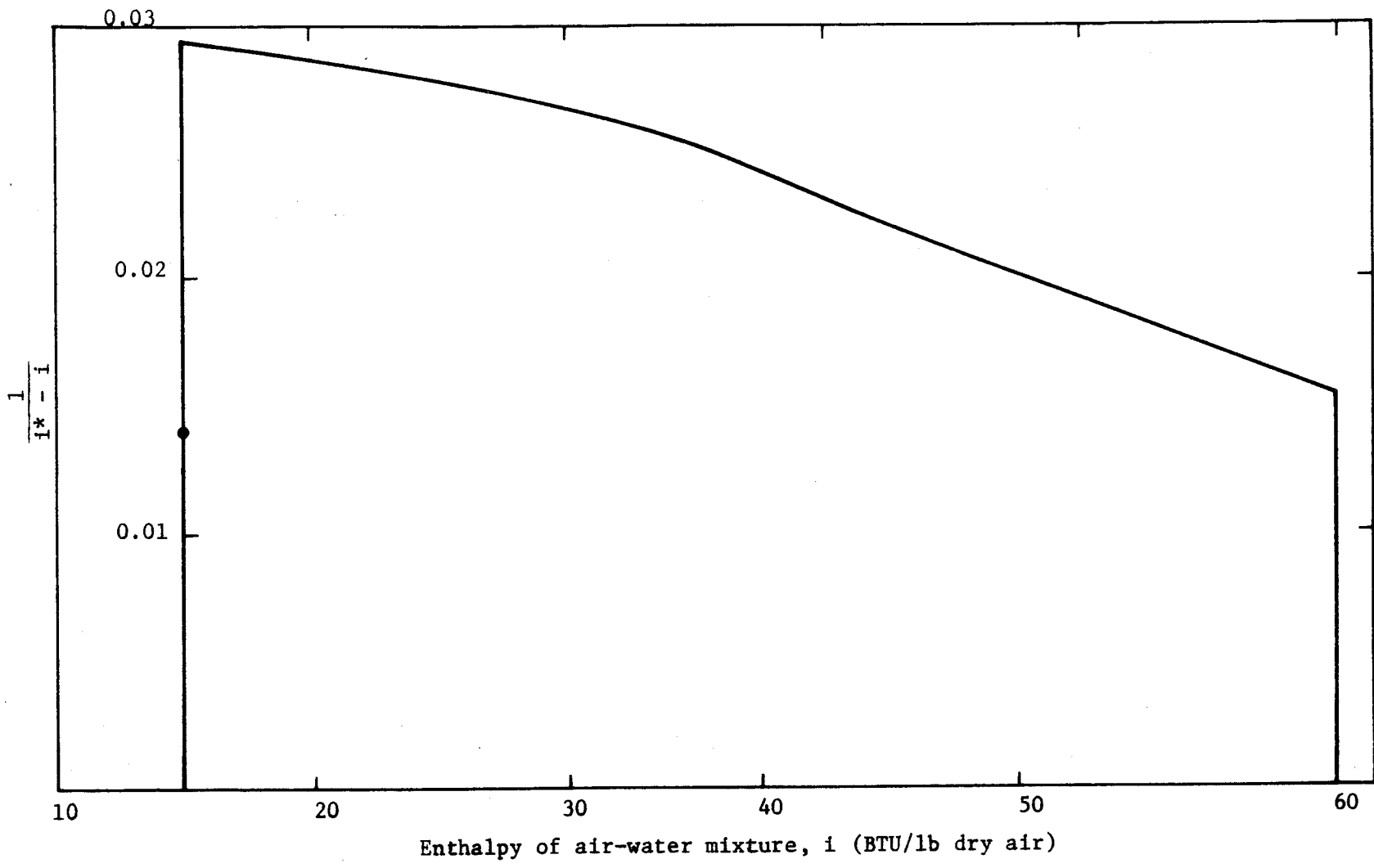


Figure 9: Graphical integration for the solution of equation 19.

planimeter and represents the intergral of equation 19. With the exception of the term $K_Y a$, all terms of equation 19 are now known. Thus, $K_Y a$, the water vapor mass transfer coefficient, can be calculated. Various values for $K_Y a$ were obtained by use of the same procedure mentioned before.

The values for $K_Y a$ computed as described above, are "apparent" values applicable to this particular column, with the high heat loss rates prevailing. If a well insulated column, with negligible heat loss, were used, considerably higher coefficients would be realized; these "adjusted" $K_Y a$ values have been calculated as follows. Assuming that heat input is equal to heat output, and estimating heat out in water and heat out in air if (1) all the heat loss had remained in water, (2) if all the heat loss had been transferred to air, the temperatures and enthalpies which would exist for both of these conditions are obtained as shown in columns (29) and (32), respectively, in Table 13. Estimating half of the heat loss through the column walls would be transferred to the air, and half would remain in the water, the data in columns (30) and (33) are obtained by averaging values in columns (3) and (29) and values in columns (14) and (32), respectively. By using the same procedure as described above for determining $K_Y a$, the adjusted operating line in Figure 8 and the adjusted $K_Y a$ values in column (34) of Table 13 are obtained. (As shown in Figure 8, the new dashed-operating line is different from the actual operating line because of the heat loss correction, while the equilibrium curve is the same for all cases).

As shown in Figure 10, the "adjusted $K_Y a$ for the packing, $(K_Y a)_P$, is related to the "apparent" $K_Y a$ for the entire apparatus, $(K_Y a)_A$, by the equation:

$$(K_Y a)_A = \theta (K_Y a)_P^\kappa \quad (21)$$

where $\kappa=1.49$ and $\theta=0.165$ as calculated by using the least squares method.

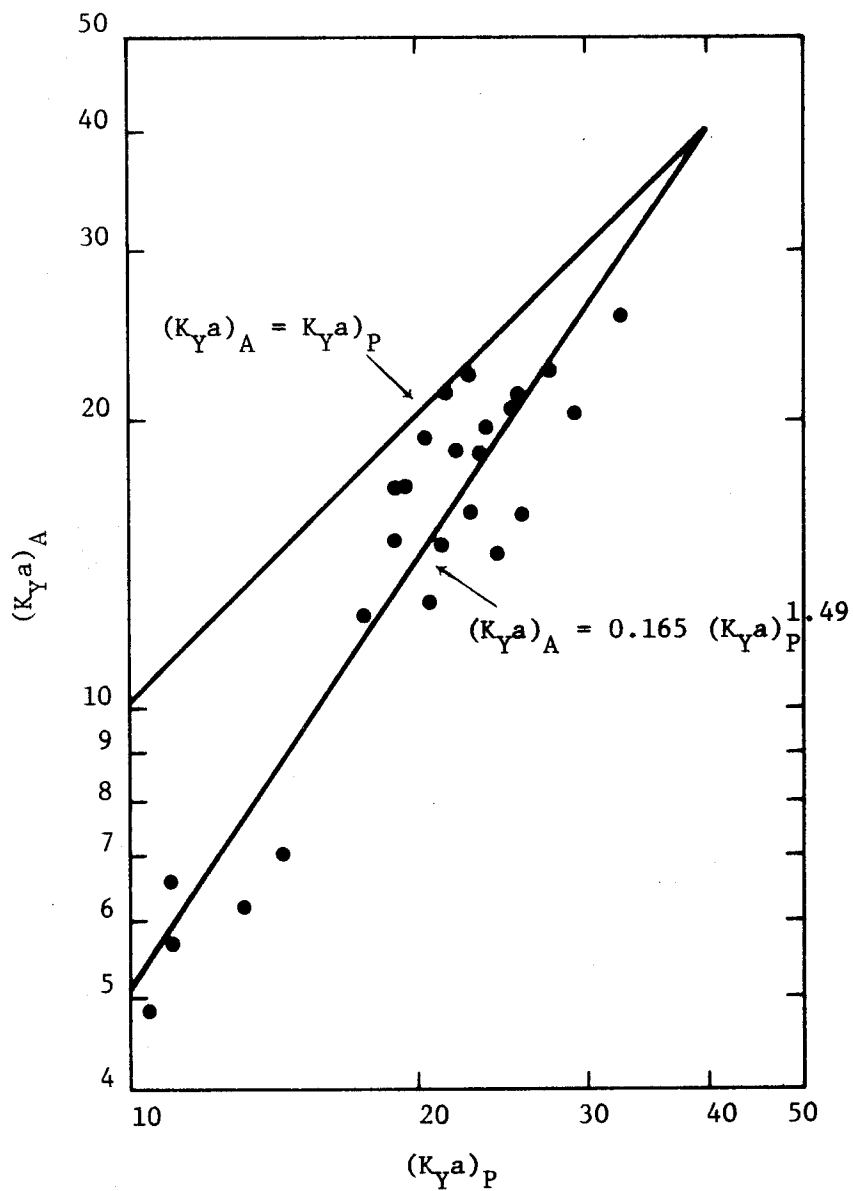


Figure 10: Relationship between the mass transfer coefficient for the apparatus and the "adjusted" values for the packing.

So equation 21 becomes

$$(K_Y a)_A = 0.165 (K_Y a)_P^{1.49}$$

i.e.

$$(K_Y a)_P = 3.35 (K_Y a)_A^{0.67} \quad (22)$$

It is clear that the mass transfer coefficient should vary with air flow rate, G , and water flow rate, L . In order to establish the quantitative relationship between these variables, the following expression is used.

$$(K_Y a)_A = \alpha (L G)^\beta \quad (23)$$

The plot of $(K_Y a)_A$ vs $(L G)$ on log-paper is shown in Figure 11, where each straight line with the same slope represents a different (L/G) ratio. Apparently, the intercept α in Figure 11 is a function of the (L/G) ratio. The slope β in equation 23 is calculated to be 0.78. So equation 23 becomes:

$$(K_Y a)_A = \alpha (L G)^{0.78} \quad (24)$$

The calculated α shown in column (37) in Table 13 (by using equation 24) vs the (L/G) ratio is shown in Figure 12. The equation in Figure 12 can be represented as follows:

$$\alpha = \phi (L/G)^\omega \quad (25)$$

where $\phi = 0.061$ and $\omega = -0.91$, are obtained by using the least squares method.

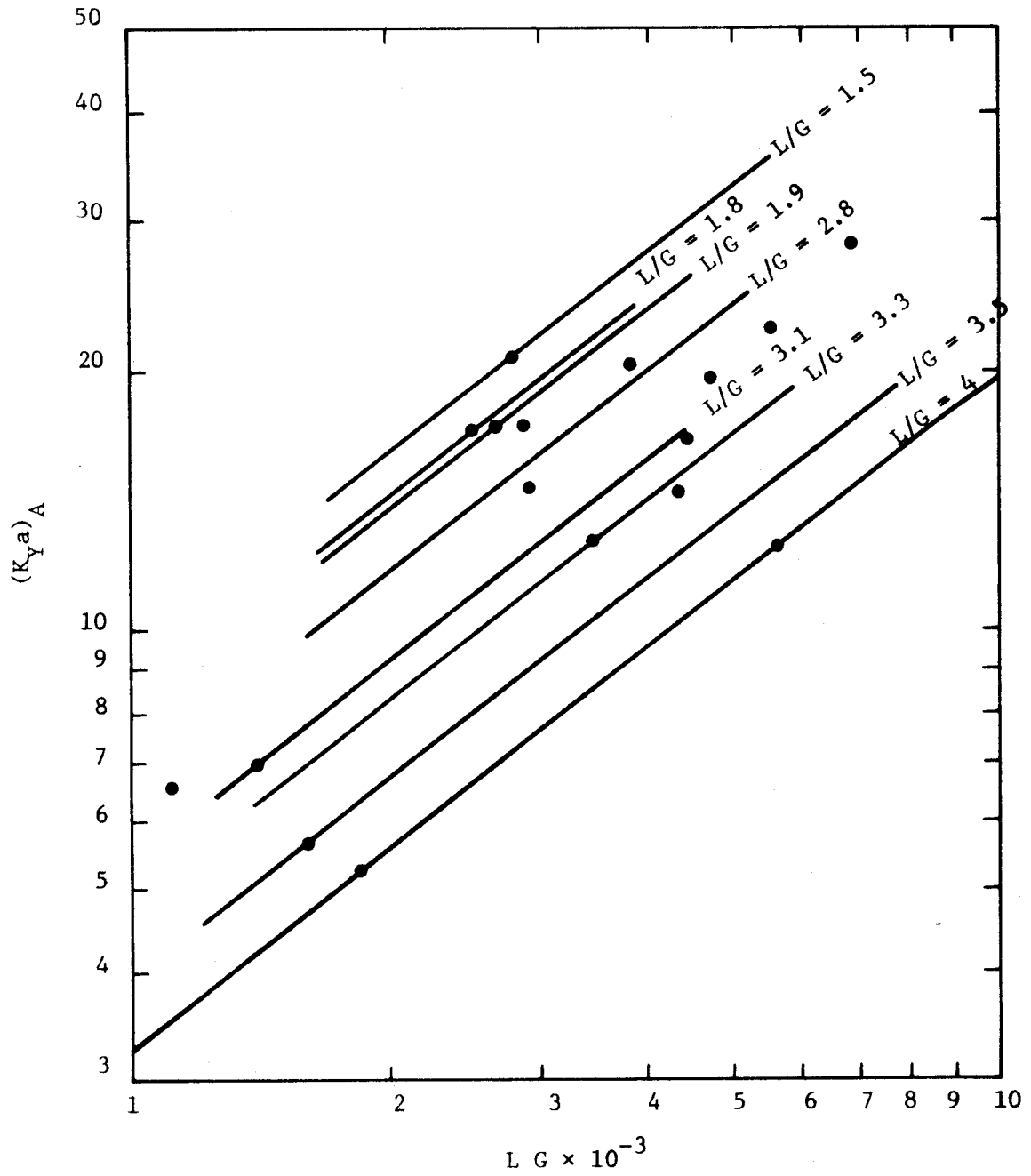


Figure 11: $K_Y a$ values for the apparatus, $(K_Y a)_A$, vs the product of air and water flow rates, $L G$.

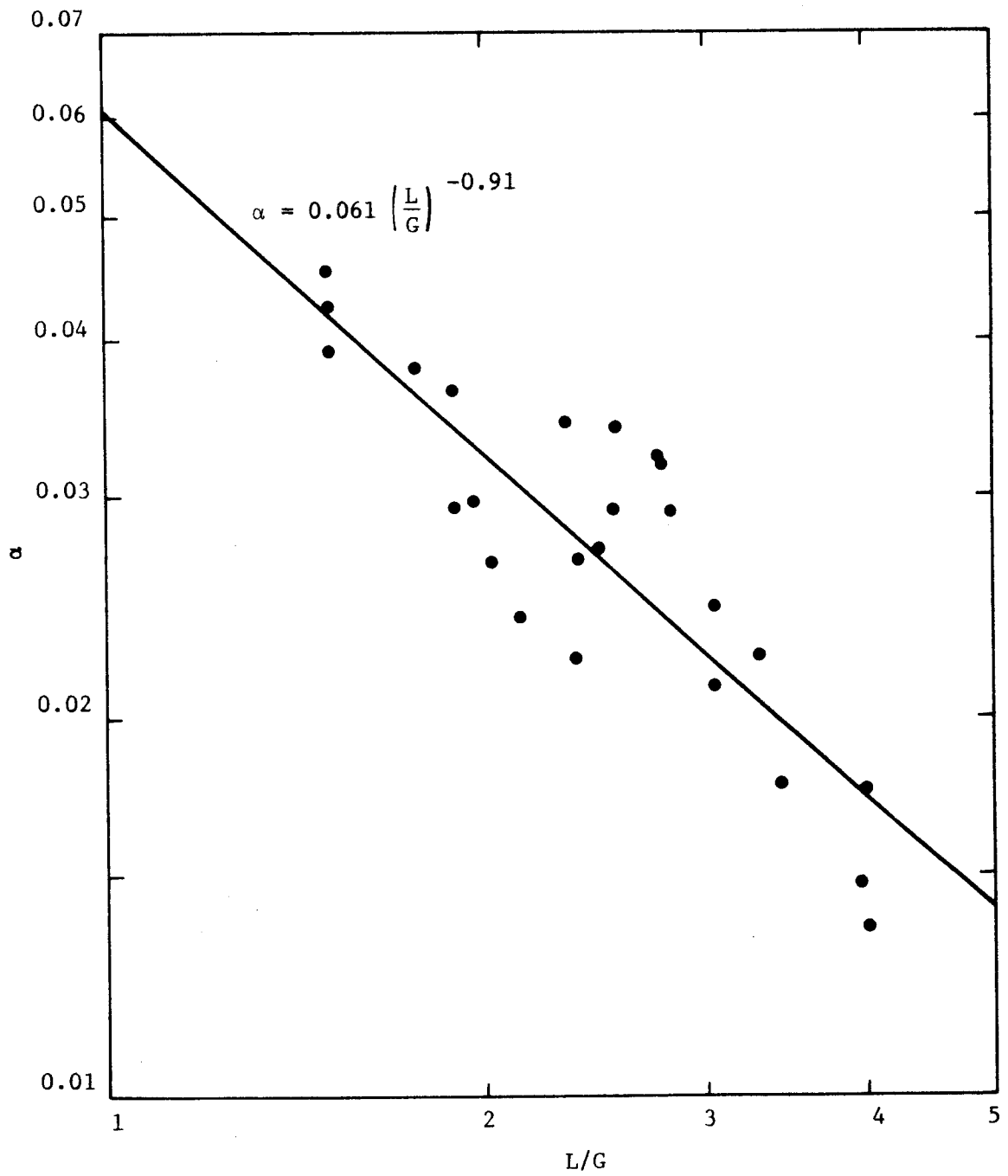


Figure 12: The constant, α , in equation 23, vs the weight ratio of water to air, L/G .

Substituting equation 25 into equation 24, the following mass transfer coefficient for the whole apparatus as a function of G and L is obtained:

$$(K_Y a)_A = \phi (L/G)^{\omega} (L G)^{0.78} = 0.061 L^{-0.13} G^{1.69} . \quad (26)$$

Combining equations 22 and 26, the mass transfer coefficient for the packing (i.e., the "adjusted" value applicable to a well insulated column) related to G and L is:

$$(K_Y a)_P = 0.51 L^{-0.087} G^{1.13} . \quad (27)$$

Comparing equation 27 with the first equation in Table 1, it is seen that the two mass transfer coefficient equations are similar even though the range of flow rates do not overlap and the packings are not the same size.

From equation 27, it appears that $K_Y a$ is practically independent of L, and approximately directly proportional to G. A plot of K_Y versus G was made by using values of K_Y shown in column (38) in Table 13 averaged for equal values of G. It was found that the data could be reasonably well correlated by the equation:

$$K_Y = 0.008 G . \quad (28)$$

If equation 27 is divided by the surface area per unit volume, $67.12 \text{ ft}^2/\text{ft}^3$, then the following equation is obtained:

$$K_Y = 0.0076 L^{-0.087} G^{1.13} . \quad (29)$$

Equations 28 and 29 are quite similar, especially when the G/L ratio is near unity. It should be recognized that these are not really

independently derived equations, both being based on the same data. In effect, equation 28 is an approximate form of equation 29.

The variation in K_Y is due in part to the fact that, at the liquid flow rates used, the packing in the column was not entirely wetted. The range for which equations 27, 28, and 29 are valid is $53 \leq L \leq 149 \text{ lb}/(\text{hr})(\text{ft}^2)$, $22 \leq G \leq 48 \text{ lb}/(\text{hr})(\text{ft}^2)$, and $0.25 \leq G/L \leq 0.66$. With the exception of the lower L value reported for the Berl saddles, the upper limits of G and L used in this study are less than the lower limits of the G and L values reported in Table 1.

Microbiology Study

The ratio of $\text{BOD}_{5\text{-day}, 20^\circ\text{C}} : \text{N} : \text{P}$ measured in the condenser water was about 160:60:1. A comparison of this ratio with the ratio of minimum nutrient requirement ($\text{BOD}:\text{N}:\text{P} = 150:5:1$) for biological treatment reported by Sawyer (34) shows that the nitrogen content, 80 percent of which is ammonia nitrogen, is quite high, while the phosphate content is at the minimum. As shown in Table 3, the addition of phosphate at a concentration of 0.37 mg/l has no obvious effect upon BOD, as the condenser water alone and that supplemented with phosphate gave similar BODs at the same temperature. In the cooling and adsorption tests in the packed column, no additions of sewage or nutrient chemicals were made.

After running the packed column a few days, there was evidence of bacterial slimes. Bacterial growth was clearly discernable around the PVC packing after two runs of condenser water

through the whole system. Each run lasted about 10 days. Each time about 120 lbs of condenser water with a sucrose concentration of 20 mg/lb of condenser water was used.

Because of the existence of a temperature gradient from the top to the bottom of the column, most of the light brown growth was found around the lower part of the column where the temperature was about 32°C. Active biological slimes also were observed between the packing and the inside surface of the column. A possible explanation for this phenomenon is that the condenser water has a greater tendency to flow down the inside surface of the column. Consequently, the concentration of the organic material is highest there and results in abundant bacterial growth.

The bacterial growth was taken from the column and was inoculated on Eosin Methylene Blue (EMB) plates, a selective medium for Gram-negative bacilli, and on Brain Heart Infusion Agar plates. All culture plates were incubated at 30°C, 37°C, 45°C, 55°C, and 65°C. No distinct difference in bacterial growth was observed at these temperatures on Brain Heart Infusion Agar plates except that at 55°C and 65°C, no growth was observed at all. Because the optimum temperature for the growth of mesophilic microorganisms lies between 30°C and 50°C, it might be expected that the bacteria are mesophiles. (Later observations showed that less growth occurred on nutrient agar slants at room temperature than at 37°C.) Because these bacteria are dependent upon organic matter for their energy, they are believed to be heterotrophic in their nutrition.

There was no growth on the EMB plates. At first glance, it leads one to suspect that all these bacteria are Gram-positive. However, most

were found to be gram negative. Since EMB medium is selective mostly for enteric gram negative bacilli, it would appear that these bacteria belong to some family other than the Enterobacteriaceae.

No growth was observed on Brain Heart Infusion Agar plates incubated anaerobically at 37°C. Because a plentiful air supply was run continuously through the packed column, it seems quite probable that no anaerobic bacteria would exist under such conditions.

After isolation of the bacteria on Brain Heart Infusion agar slants, microscopic examination was made. The description of bacteria is shown in Table 14. In order to identify these bacteria, many biochemical tests were performed, including fermentation of different carbohydrates, reaction in litmus milk, production of hydrogen sulfide and indole, reduction of nitrate and gelatin liquefaction. All these biochemical activities were negative. In other words, these bacteria are so inactive that they do not respond to these different biochemical tests.

Table 14: Characteristics of Bacteria

Bacteria number	Description on agar plate	Gram-Stain	Description of microscopic observation
1	small, yellow, raised	(+)	fusiform shaped rods, pleomorphic, slender, long, short and plump
2	medium, pink, smooth periphery	(-)	tiny rods in pairs, short chains
3	large, yellow-white	(-)	tiny rod
4	small, yellow-white	(-)	slender rods

In the experiment which used the cooling column as a trickling filter, it was evident that these bacteria were able to oxidize the organic matter, most of which was expected to be sucrose. The failure of these same bacteria to cause fermentation in various sugars necessitated a search for an oxidation medium. Therefore OF Basal medium was used to see if these bacteria could oxidize sucrose. Experimental results showed positive reactions in sucrose oxidation.

When one considers the conditions under which the experiment was conducted (continuous inflow of air), it is not surprising to find that these bacteria only oxidize rather than ferment the sucrose. Thus, it would appear that oxygen rather than some organic compound is the terminal electron acceptor. What was rather unusual was that four of the organisms utilized sucrose but no glucose. With most bacteria, sucrose would be converted to glucose and then glucose would be broken down in one of the known pathways for glucose catabolism.

From an examination of Bergey's Manual (35), one could suggest tentatively that organisms 1 and organisms 2 to 4 in Table 14 would be members of the families of Corynebacteriaceae and of Achromobacteriaceae, respectively. An objection to these suggested families is that some of the optimum temperatures should be at room temperature. Because the temperature of the cooling column was always above room temperature, it may be that the organisms mutated to adapt themselves to the higher temperature. Bacteria are known to adapt and mutate rather easily.

CHAPTER VI

SUMMARY AND CONCLUSION

The following conclusions can be made concerning this dual cooling-purification process in a packed column.

1. A packed column can be employed for cooling beet sugar factory condenser water effluent while simultaneously removing organic matter by biological oxidation.

2. No objectional odors or other nuisances were found in this aerobic system.

3. Biological growth in this experiment was automatic and self-perpetuating. No additional chemicals or domestic sewage had to be added as nutrients to the condenser water from the beet sugar factory. It appears that the condenser water effluent contained nutrients which provided a balanced microbial diet. The excess supply of oxygen and optimal temperature could account for this spontaneous, rapid biological growth. Four principal microorganisms were found to be present; these organisms were responsible for the degradation of the adsorbed organic matter in the beet sugar factory condenser water effluent.

4. Biological growth was found on PVC Raschig rings. Consideration of the low cost and large surface area/unit volume of these rings shows them to be a good filling material in biological wastewater treatment. The surface area/unit volume for the 0.84 inch Raschig rings used in this study is $67.12 \text{ ft}^2/\text{ft}^3$, compared to 14 ft^{-1} for the rocks and fieldstones usually used in trickling filters.

In a trickling filter and cooling tower, it is desirable to maximize the surface area per unit volume. On the other hand, the pore cross section must be large enough to permit the passage of sloughed slime growth without plugging (in a cooling tower, the pore cross section must be large enough so that there is not excessive head loss). Listed in Table 15 are the properties of some geometric shapes that could be considered as possible media for a combination trickling filter and cooling tower.

5. It is possible to reuse this treated condenser water. The recirculation of this water would reduce the withdrawals of fresh water for beet sugar plant operation and would reduce thermal and organic pollution from this effluent.

6. The semi-empirical equation of detention time related to water velocity and air-water weight ratio is valid when this ratio is less than 0.4:

$$t = 0.1137 \text{ h} \left(\frac{v}{g} \right)^{1/3} \left(\frac{A/V}{Q} \right)^{2/3} + 400 \text{ (G/L)} \quad (18)$$

7. The empirical equation for the mass transfer coefficient is:

$$K_Y a = 0.51 \text{ L}^{-0.087} \text{ G}^{1.13} \quad (27)$$

8. The empirical equation for the mass transfer film coefficient (gas phase) for Raschig rings is:

$$K_Y = 0.0076 \text{ L}^{-0.087} \text{ G}^{1.13} \text{ or approximately}$$

$$K_Y \approx 0.008 \text{ G.}$$

Table 15: The Packing Properties of Some Geometric Shapes

Reference	Geometric Shape	Nominal Size (in.)	Wall Thickness (in.)	Number per ft ³ of Bed Volume (#/ft ³)	Surface Area per Bed Volume (ft ² /ft ³)	Porosity	Weight Density (lb/ft ³)
	Raschig rings used in this study	0.84	0.08	2,300	67.12	0.85	17.6
36	Metal Raschig ring rings	0.75	0.0625	3.190	71.8	0.78	100
37	Rocks and fieldstone	3.2			14	0.4	
36	Carbon Raschig rings	1	0.125	1,325	57	0.74	27
36	Ceramic Lessing rings	1	0.125	1,300	69	0.66	50
36	Cross-partition rings	3	0.312	74	43	0.49	73
36	Cyclohelix spiral rings	4	0.267	31	40	0.53	65
36	Berl Saddle packings	1		2,200	76	0.69	45
36	Intalox Saddle packings	1		2,385	78	0.775	34

9. % COD removal per effective pass (P/F) ranged from 11% to 52% at COD loading rates of 0.025 and 0.011 lbs COD/(hr)(ft²), respectively. Most of the NH₃ removal is by air stripping rather than by oxidation. Because most of the nitrogen in condenser water exists in the form of ammonia (introduced by evaporating and cooling operations), the removal of nitrogen centers on the removal of ammonia nitrogen.

LIST OF SYMBOLS

<u>Symbol</u>	<u>Definition</u>	<u>Dimension</u>	<u>Units</u>
A/V	Surface area/unit volume of bed	1/L	1/ft
BOD	Biochemical Oxygen Demand	M/L ³	mg/l
BTU	British thermal unit	ML ² /T ²	BTU
c	Constant that reflects film build-up	dimensionless
c	Final COD concentration	M/L ³	mg/l
c ₀	Initial COD concentration	M/L ³	mg/l
°C	Centigrade temperature	ML ² /T ²	°C
COD	Chemical Oxygen Demand	M/L ³	mg/l
c _s	Humid heat	T ² /ML	$\frac{\text{BTU}}{(\text{°F})(\text{lb dry air})}$
DO	Dissolved oxygen	M/L ³	mg/l
°F	Fahrenheit temperature	ML ² /T ²	°F
g	Acceleration of gravity, 32.2 ft/sec ²	L/T ²	ft/sec ²
G'	Air flow rate	ML/T ³	lb/hr
G	Superficial velocity of air	M/LT ³	lb/(hr)(ft ²)
G/L	Weight rate ratio of air to water	dimensionless	$\frac{\text{lb of air/hr}}{\text{lb of water/hr}}$
gpm	Flow rate	L ³ /T	gal/min
h	Depth	L	ft
H	Humidity	dimensionless	$\frac{\text{lb of water vapor}}{\text{lb of dry air}}$
H*	Saturation humidity	dimensionless	$\frac{\text{lb of water vapor}}{\text{lb of dry air}}$
ΔH	Humidity difference	dimensionless	$\frac{\text{lb of water vapor}}{\text{lb of dry air}}$

<u>Symbol</u>	<u>Definition</u>	<u>Dimension</u>	<u>Units</u>
i	Enthalpy of air-water mixture	L	BTU/lb dry air
i*	Enthalpy of a saturated air-water mixture in equilibrium with the bulk of water	L	BTU/lb dry air
i_1, i_2	Enthalpy of the inlet and outlet air, respectively	L	BTU/lb dry air
k	Proportionality factor in equation 2	1/T	1/time
k	BOD rate constant	1/T	1/days
k	Order in table 6	dimensionless
k	Constant in equation 14	dimensionless
K	The fraction of the pore volume occupied by the liquid in equation 14	dimensionless
$k_{1,5}$	BOD rate constant	1/T	1/days
K_Y	Mass transfer coefficient for Raschig rings	M/T ³ L	$\frac{\text{lb}}{(\text{hr})(\text{ft}^2)(\Delta H)}$
K_{Ya}	Overall volumetric mass transfer coefficient	M/T ³ L ²	$\frac{\text{lb}}{(\text{hr})(\text{ft}^3)(\Delta H)}$
n	A measure of the degree of dropoff in treatment response	dimensionless
L'	Water flow rate	ML/T ³	lb/hr
L	Superficial velocity of water	M/LT ³	lb/(hr)(ft ²)
L	The initial or first-stage BOD of the wastewater	M/L ³	mg/l
M	Mean value in table 6	dimensionless
L/G	Weight rate ratio of water to air	dimensionless
Q	Flow rate	L/T	ft/sec
t	Time for BOD exertion	T	days

<u>Symbol</u>	<u>Definition</u>	<u>Dimension</u>	<u>Units</u>
t	Detention time with air flow	T	seconds
t_d	Detention time without air flow	T	seconds
Δt	Increased detention time	T	seconds
TOD	Theoretical oxygen demand	M/L ³	mg/l
TDS	Total dissolved solids	M/L ³	mg/l
w	Final condenser water weight	ML/T ²	lb
w_o	Initial condenser water weight	ML/T ²	lb
Δw	Condenser water added	ML/T ²	lb
x	Difference between mean value and COD/BOD _{5-day, 20°C}	dimensionless
X	COD/BOD _{5-day, 20°C}	dimensionless
y	The amount removed during passage through the treatment system	M/L ³	mg/l
y_o	Initial amount of substances present in the applied water	M/L ³	mg/l
Z	Height of the packing column	L	ft
$\alpha, \beta, \theta, \kappa,$	Constants
ν	Kinematic viscosity	L ² /T	ft ² /sec
δ	Standard deviation	dimensionless

BIBLIOGRAPHY

1. S.L. Force, "Beet Sugar Factory Wastes and Their Treatment Primarily the Findlay System," Proceedings of the 7th Industrial Waste Conference, Purdue University, no. 113, pp. 116-122, (March, 1962).
2. H.F. Elkin, "Biological Oxidation and Re-use of Refinery Wastewater for Pollution Contrl." Proceedings of the American Petroleum Institute, (May, 1956) 6 pages.
3. H.F. Elkin, E.F. Mohler, and L.R. Kumnick, "Biological Oxidation of Oil Refinery Wastes in a Cooling Tower System." Sewage and Industrial Wastes, volume 28, no. 12, p. 1478 (December, 1956).
4. H.F. Elkin, "Purify While They Cool." American Petroleum Institute Meeting, (May, 1956) 4 pages.
5. J.C. Reynolds, "Staley Saves Water, Cuts Process Waste." Power Engineering, pp. 88-90, (February, 1959).
6. R.M. Smith, "Use of a Cooling Tower as a Trickling Filter in Pollution Control." Cooling Tower Institute Meeting, (January 28, 1964), 16 pages.
7. E.F. Mohler, H.F. Elkin, and L.R. Kumnick, "Extended Experience with Reuse and Bio-oxidation of Refinery Wastewater in Cooling Tower System." 37th Annual Ohio Water Pollution Control Conference, (June 13, 1963), 13 pages.
8. F. Yoshida, and T. Tanaka, "Air-Water Contact Operations in a Packed Column." Industrial and Engineering Chemistry, volume 43, no. 6, pp. 1467-1473, (June, 1951).
9. S.L. Hensel, and R.E. Treybal, "Air-Water Contact-Adiabatic Humidification of Air with Water in Packed Tower." Chemical Engineering Progress, volume 48, pp. 362-370, (1952).
10. J. Lichtenstein, "Performance and Selection of Mechanical-Draft Cooling Towers." American Society of Mechanical Engineering, Transactions, volume 65, pp. 779-787, (1943).
11. W.M. Simpson, and T.K. Sherwood, "Performance of Small Mechanical Draft Cooling Towers." Refrigerating Engineering, volume 52, pp. 535-543, (December, 1946).
12. L.G. Rich, Unit Processes of Sanitary Engineering, John Wiley and Sons, Inc., New York, 1963, p. 47.

13. G.M. Fair, and J.C. Geyer, Water Supply and Wastewater Disposal, John Wiley and Sons, Inc., New York, 1954, page 703.
14. G.M. Fair, J.C. Geyer, and D.A. Okun, Water and Wastewater Engineering, Volume 2, Water Purification and Wastewater Treatment and Disposal, John Wiley and Sons, Inc., New York, 1968, page 35-6.
15. Ibid, page 34-12.
16. J.A. Popter, P.H. Dutch, "Phenol-Cyanide Removal in a Plastic-Packed Trickling Filter." Journal Water Pollution Control Federation, volume 32, no. 6, p. 622, (June, 1960).
17. H.W. Gehm, and I. Gellman, "Practice, Research, and Development in Biological Oxidation of Pulp and Papermill Effluents." Journal Water Pollution Control Federation, volume 37, no. 10, p. 1392, (October, 1965).
18. "Cooling Towers Resist Corrosion," Water and Waste Treatment, March/April, 1967, p. 268.
19. K.R. Devones, D.R. Fisher, and O.P. Morgan, "Experience with Low Rate Biological Treatment Processes." Proceedings of the 23rd Industrial Waste Conference, Purdue University, no. 132, p. 10, (May, 1968).
20. Reference 14, p. 33-11.
21. G.M. Fair, "The Log-Difference Method of Estimating the Constants of the First-Stage Biochemical Oxygen Demand Curve." Sewage Works Journal, volume 8, no. 3, p. 430, (May, 1936).
22. H.A. Thomas, Jr., "The Slope Method of Evaluating the Constants of the First-Stage Biochemical Oxygen Demand Curve." Sewage Works Journal, volume 9, no. 3, p. 425, (May, 1937).
23. E.W. Moore, H.A. Thomas, Jr., and W.B. Snow, "Simplified Method for Analysis of BOD Data." Sewage and Industrial Wastes, volume 22, no. 10, p. 1344, (October, 1950).
24. J.D. Lee, "Simplified Method for Analysis of BOD Data." Sewage and Industrial Wastes, volume 23, no. 2, p. 164, (February, 1951).
25. J.P. Sheehy, "Rapid Methods for Solving First-Order Equations." Journal Water Pollution Control Federation, volume 32, no. 6, p. 646, (June, 1960).
26. J.C. Ward, and E.M. Jex, "Characteristics of Aqueous Solutions of Cattle Manure." Presented at the Cornell University Agricultural Animal Waste Conference, Syracuse, New York, January 13-15, 1969, pp. 310-326.

27. Reference 12, p. 8.
28. Reference 14, p. 22-16.
29. Ibid, p. 22-17.
30. W.F. Howland, "Flow Over Porous Media as in a Trickle Filter." Proceedings of the 12th Industrial Waste Conference, Purdue University, volume 12, p. 435, (1957).
31. Reference 14, p. 27-16.
32. H. Sawistowski, and W. Smith, Mass Transfer Process Calculation, John Wiley and Sons, Inc., New York, 1963, p. 18 and 430.
33. L.G. Rich, Unit Operation of Sanitary Engineering, John Wiley, and Sons, Inc., New York, 1961, p. 265.
34. Reference 14, p. 34-6.
35. Bergey's Manual of Determinative Bacteriology, 7th Edition, The Williams and Wilkins Co., Baltimore, 1957.
36. M. Leva, Tower Packings and Packed Tower Design, The United States Stoneware Company, Akron, Ohio, pp. 7-14, (December, 1953).
37. Reference 14, p. 35-7.

APPENDIX

CALCULATION AND DATA FOR TABLE 4

Fair's Log Difference Method

(1)	(2)	(3)	(4)	(5)
t	y	d		
Time in days	BOD (mg/l) observed in stated time	BOD increment	log d	t log d
1	14.5	14.5	1.161	1.161
2	21.5	7	0.845	1.690
3	27	6.5	0.813	2.439
4	32	5	0.699	2.796
5	37	5	0.699	3.495
Σ			4.217	11.581

$$k = 0.107$$

Thomas' Slope Method

(1)	(2)	(3)	(4)	(5)
t	y	*y'	yy'	y ²
Time in days	BOD (mg/l) observed in stated time			
1	14.5	10.75	155.875	210.25
2	21.5	6.25	134.375	462.25
3	27	5.25	141.750	729.00
4	32	5	160.000	1024.00
5	37	4.5	166.500	1369.00
Σ	132	31.75	758.5	3794.5

$$\text{where } y' = \frac{y_{i+1} - y_{i-1}}{t_{i+1} - t_{i-1}}$$

$$k = 0.112$$

Moore's Moment Method

(1) t	(2) y	(3) ty
Time in days	BOD (mg/l) observed in stated time	
1	14.5	14.5
2	21.5	43
3	27	81
4	32	128
5	37	185
Σ	132	451.5

from the chart (reference 23); $k = 0.160$

Lee's Method

With the plot of observed BOD on special paper with exponential time scale, (Figure 1, p. 165, reference 24) and semilogarithmic plot used to find k (Figure 2, p. 165, reference 24), the k value is calculated to be 0.135

Sheehy's Graphical Method

With the Figure 2 (p. 648, reference 25), the $k_{2,5}$ is equal to 0.13

(Based on $\frac{\text{BOD}_{2\text{-day}}}{\text{BOD}_{5\text{-day}}}$ calculation).